UNIVERSITY OF NAPLES FEDERICO II

PH.D. PROGRAM IN

CLINICAL AND EXPERIMENTAL MEDICINE

CURRICULUM IN TRANSLATIONAL MEDICAL SCIENCES

XXXVI Cycle

(Years 2020-2023)

PH.D. THESIS

IL-33 STIMULATES THE ANTICANCER ACTIVITIES OF EOSINOPHILS THROUGH EXOSOME-MEDIATED REPROGRAMMING OF TUMOR CELLS

TUTOR

Prof. Stefania Loffredo

PH.D. STUDENT

Dr. Adriana Rosa Gambardella

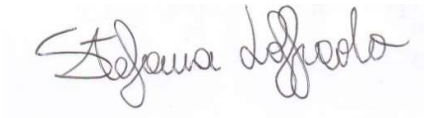

SUPERVISOR

Dr. Giovanna Schiavoni

1. INTRODUCTION

1.1 *IL-33*

Interleukin (IL)-33 is an epithelial-derived 'alarmin' for the immune system that can be released upon tissue damage, stress or infection. It was initially described as a nuclear factor associated with chromatin that binds H2A and H2B histones (Roussel et al., 2008). IL-33 belongs to the IL-1 family of cytokines and it is involved in different immune processes: *i)* inflammatory diseases, *ii)* allergies, *iii)* infections and *iiii)* cancer (Liew et al., 2016). IL-33 is expressed by a number of cell types, such as endothelial cells, fibroblasts, epithelial cells and other stromal cells (Andreone et al., 2020; Cayrol et al., 2018). IL-33 binds to a heterodimer formed by its primary receptor ST2 and the co-receptor IL-1 receptor accessory protein (IL1RAP). This interaction activates the nuclear factor kappa-light-chain-enhancer of activated B cells (NF-kB), c-Jun N-terminal kinase (JNK) and mitogen-activated protein kinase (MAPK) signaling through a MyD88-IRAK-dependent pathway. This results in the release of a plethora of soluble mediators by different immune cells (Drake et al., 2017). IL1RAP is constitutively expressed at low levels by all cells, including immune cells (Boraschi et al., 2018) while ST2 is expressed primarily by cells that act in Th2 responses, such as eosinophils, basophils, mast cells, T regulatory cells (Treg) and type 2 innate lymphoid cells (ILC2) and secondarily by T helper (Th) 1 cells, $CD8^+$ T cells, natural killer (NK) cells, macrophages, neutrophils, dendritic cells (DCs) and B cells (Afferni et al., 2018; Lu et al., 2015). Therefore, IL-33 has the capacity to stimulate both Th2 and Th1-type of immune responses (Mattei et al., 2020). IL-33 displays multiple functions in a wide variety of pathologies, such as allergy, cardiovascular diseases, chronic obstructive pulmonary disease (COPD), fibrotic diseases, musculoskeletal diseases, inflammatory bowel diseases, diseases of the central nervous system (Alzheimer), obesity, diabetes and cancer (Liew et al., 2016).

1.2 *IL-33 and cancer*

IL-33 has a controversial role in cancer immunity. Both pro- and anti-tumoral functions have been reported depending on the tumor type and the specific microenvironment. In breast cancer mouse models, the IL-33/ST2 axis promotes the growth as well as lung

and liver metastases of 4T1 mammary tumors facilitating the intratumoral accumulation of immunosuppressive cells, such as myeloid Gr-1$^+$ tumor growth factor (TGF) -β1$^+$ myeloid -derived suppressor cells (MDSCs), IL-10-expressing CD11c$^+$ DCs, alternatively activated M2 macrophages, ILC2 and Treg cells, while dampening the expansion of activated NK cells (Jovanovik et al., 2014). It was also observed that in colorectal cancer IL-33 promotes tumorigenesis and tumor progression (Akimoto et al., 2018). Conversely, in a murine model of acute myeloid leukemia (AML), the administration of IL-33 significantly inhibited leukemia growth and improved mice survival rate in a CD8$^+$ T cell dependent manner (Spits et al., 2013).

Moreover, the combination of programmed cell death 1 (PD-1) checkpoint blockade with IL-33 prolonged mice survival and induced complete leukemia regression in 50% of animals (Duault et al., 2017). In a human papilloma virus (HPV)-associated model for cancer immunotherapy, IL-33 acts as a potent vaccine adjuvant augmenting Th1 and CD8$^+$ T-cell responses, leading to regression of established TC-1 tumors in mice (Villarreal et al., 2014). In an acute myeloid leukemia (AML) model, IL-33 treatment significantly increased the percentage of effector memory liver CD8$^+$ T cells, leading to delayed leukemia development and improved overall survival (Qin et al., 2016). Lucarini et colleagues demonstrated that in mice IL-33 inhibits melanoma tumor growth and pulmonary metastasis in an eosinophil-dependent manner. They observed increased metastatic load and reduced lung eosinophilia in ST2-deficient compared to wild type (WT) mice and that the depletion of eosinophils completely abolished the anti-tumor effects of IL-33 administration (Lucarini et al., 2017). Moreover, overexpression of IL-33 was reported to inhibit tumor metastasis in the B16 melanoma model (Gao et al., 2013).

The axis IL-33/ST2 might be considered as a predictive biomarker of tumor progression and patient survival. There is a positive correlation between IL-33 expression in tumor tissues and positive outcomes in cancer patients. In fact, it was reported that IL-33 and ST2 levels were up-regulated in non-transformed lung cells and were significantly downregulated in both adenocarcinoma and squamous cell carcinoma of lung tissues (Yang et al., 2018). Plasma IL-33 levels were elevated during the early stage of lung cancer and decreased with advanced cancer stages, probably due to lung volume reduction containing bronchial epithelium and vascular endothelium as sources of IL-33 (Kim et al., 2015). Tumor, epithelial and immune cells express the soluble form of ST2 (sST2) at various levels, which may contribute to regulate the availability of IL-33 in

the tumor microenvironment (TME), modulating tumor immunity (Chang et al., 2020). The current literature suggests that the anti-tumor functions of IL-33 can be attributed to its ability to stimulate immune cells (such as $CD8^+$ T cells, NK, DCs, eosinophils and ILC2). Immune cell activation plays a fundamental role in the first containment of tumor development through the secretion of several soluble mediators that orchestrate tumor immunity by recruiting cells responsible for the initiation of adaptive responses (Varricchi et al., 2017; Marone et al., 2020; Mattei et al., 2020; Ercolano et al., 2019).

1.3 *Eosinophils*

Eosinophils (Eo) are a rare blood-circulating and tissue-infiltrating innate immune cell population representing 1–3% of total granulocytic leukocyte under physiological condition (Mattei, 2020). These granulocytes are known to originate and differentiate in the bone marrow (BM) in response to IL-5, IL-3 and granulocyte and monocyte colony stimulating factor (GM-CSF), which support both maturation and survival of Eo (Ghaffari et al., 2023). Upon response to certain inflammatory conditions (i.e., allergies, parasitic infections, and autoimmune diseases), Eo can rapidly expand and infiltrate inflamed tissues, where they play diverse roles in inflammatory responses due to Th2 functions. Eo can carry out *i)* effector functions, *ii)* tissue remodeling, *iii)* cell interactions and *iiii)* immunomodulation (Shamri et al., 2011).

As an innate immune cell, Eo exhibit antibacterial (Arnold et al., 2018), antiviral (Phipps et al., 2007), antiparasitic (Hogan et al., 2008) and anti-tumor effector activities (Andreone et al, 2019; Jia et al., 2019; Lucarini et al., 2017; Varricchi et al., 2017). Their cytoplasm is characterized by multi-lobated nucleus and by the presence of lytic granules that contain cytotoxic proteins (Granzyme B; EPX, Eo-peroxidase; ECP, Eo cationic protein) which mediate the cytotoxic functions of Eo through degranulation. After activation with endogenous alarmins, pathogen- and damage-associated molecular signals or cytokine stimulation, Eo migrate through the bloodstream to inflamed sites. Activated Eo exhibit increased survival and expansion, high adhesion receptor activation and finally release stored mediators (Kvarnhammar et al., 2012; Arnoult et al., 2011). Recent evidences demonstrated that IL-33 constitutes a potent stimulus that sustains eosinophilopoiesis at various levels, promoting Eo survival and, indirectly, Eo recruitment, via stimulation of tumor cell-derived chemokines. IL-33 activates Eo

directly, up-regulating CD69, the adhesion molecules intercellular adhesion molecule (ICAM)-1 and CD11b/CD18 and the degranulation marker CD63 (Andreone et al., 2019). In the steady state, resident Eo perform functions related to tissue development/maintenance, tissue regeneration and remodeling, metabolism and immune homeostasis, all of which are integral to innate immunity (Ghaffari et al., 2023).

1.4 *Eosinophils and cancer*

An increasing number of studies have highlighted an important role of Eo in cancer. As mentioned above, these cells secrete a wide array of soluble mediators and effector molecules that are involved in immunoregulatory activities and/or cancer immunity in the TME (Mattei et al., 2020). Reportedly, these granulocytes are known to infiltrate most tumors and this evidence has given importance to these cells in the context of TME. This condition is referred to as tumor-associated tissue eosinophilia (TATE) which may have prognostic and predictive role in human cancers (Simon et al., 2019; Varricchi et al., 2018). Pro-tumoral functions of Eo were described in cervical carcinoma patients where high percentage of TATE correlate with a less effective antitumor response and a worse overall survival (Xie et al., 2015). In hematological tumors, such as Hodgkin' lymphoma and T-cell leukemia/lymphoma, Eo constitute an unfavorable prognostic factor for overall survival (Von Wasielewski et al., 2000; Enblad et al., 1993; Utsunomiya et al., 2007).

By contrast, several studies highlight the anti-tumor activity of Eo, considering their presence in peripheral blood or in TME as a favorable prognostic factor. Recent clinical observations in melanoma patients undergoing immunotherapy, targeting the immune checkpoints cytotoxic T-lymphocyte antigen 4 (CTLA-4) and PD-1, have unraveled a predictive role of Eo counts for therapeutic response (Buder-Bakhaya et al., 2018). Further evidences reported that, in melanoma, the treatment with pembrolizumab (PD-1 antibody) or the synergistic activity of nivolumab (anti-PD-1) and ipilimumab (anti-CTLA-4) increases Eo number both in TME and peripheral blood, together with an increase of tumor-infiltrating $CD8^+$ T cells, indicating the effectiveness of immunotherapy (Simon et al., 2020). It has been recently reported that IL-33 activated Eo can perform direct anti-tumor activity through the release of Eo cationic/cytotoxic proteins contained in their granules. Andreone and colleagues elegantly demonstrated that, upon activation with IL-33, Eo exert cytotoxic functions against several tumor cell

lines through CD11b/CD18 integrin complex and synapse polarized degranulation, resulting in tumor cell apoptosis (Andreone et al., 2019).

Moreover, Eo were reported to exert cytotoxic activity against colorectal cancer, in a $CD8^+$ T cell independent manner (Reichman et al., 2019). Eo may promote anti-tumor immunity triggering direct tumor cell killing or through the interaction with other immune cells in TME. In breast cancer is demonstrated that Eo, infiltrating lung metastases, can promote $CD4^+$ and $CD8^+$ T cell recruitment (Grisaru-Tal et al., 2021). Eo and T cells synergize to promote up-regulation of vascular cell adhesion molecule (VCAM)-1 expression, decreasing hypoxia, increasing vascular profusion and polarization of tumor-associated macrophages towards the M1 phenotype expressing low levels of pro-angiogenic factors, such as vascular endothelial growth factor (VEGF) (Carretero et al., 2015).

1.5 *Exosomes*

Exosomes (Exo) are nanosized (30-150 nm) extracellular vesicles (EVs) secreted by all cell types that play central roles in intercellular communication in health and disease. Exo are membrane bound carriers that transfer their molecular bioactive cargo that consists of nucleic acids, proteins, lipids and metabolites and that reflects the nature of donor cell and its physiological state, to recipient cells inducing downstream signaling cascades (Deatherage et al., 2012; Doyle et al., 2019). Although initially identified as a cellular mechanism to excrete unwanted cellular products, Exo are now known to influence a broad range of physiological processes such as immune responses (Nolte-'t Hoen et al., 2009), tissue repair (Zhang et al., 2015; Cui et al., 2017), stem cell maintenance (Ratajczak et al., 2006), central nervous system diseases (Men et al., 2019) and pathological processes in cardiovascular diseases (Bang et al., 2014; Zamani et al., 2019), neurodegeneration (Howitt et al., 2016), cancer (Osaki et al., 2019) and inflammation (Deng et al., 2009). The rigid bilayer membrane of Exo includes lipid components, such as sphingomyelin, cholesterol and ceramides, which influence cargo sorting, Exo secretion, structure and signaling (Skotland et al., 2019).

Exo are present in various biological fluids (breast milk, blood, serum, urine, saliva, amniotic and synovial fluids) and might undergo multiple cell uptake and release cycles to allow access to several layers of tissues (Lakhal et al., 2011). Several studies demonstrated that both cell-derived and body fluid-derived Exo show tropism to most

organs, such as liver, lung, kidney, pancreas, spleen, ovaries, colon and brain after oral administration. Intravenous administration, by contrast, causes a predominant Exo sequestration in the liver, spleen, lungs and the gastrointestinal tract (Murphy et al., 2019). Proteins, metabolites and nucleic acids delivered by Exo into recipient cells can effectively alter their biological response. Exo-mediated responses can be disease promoting or restraining (Kalluri et al., 2016). The intrinsic properties of Exo in regulating intracellular pathways have advanced their potential utility in the therapeutic control of many diseases, including cancer.

1.6 *Exosome biogenesis*

Exo biogenesis is preceded by endocytosis, whereby the plasma membrane invades the cytoplasm and then forms a cup-shaped structure resulting in the formation of early endosomes that incorporate a molecular cargo into intraluminal vesicles (ILVs) forming multivesicular bodies (MVBs), a subset of specialized endosomal compartments rich in ILVs which sequester specific proteins, lipids and cytosolic components (Gurung et al., 2021). MVBs are transported to the plasma membrane via cytoskeletal and microtubule network and undergo exocytosis post fusion with plasma membrane whereby the ILVs are secreted as Exo into the extracellular space.

Multiple mechanisms involved in Exo biogenesis have been identified. ILVs biogenesis and secretion are driven by the endosomal sorting complex required for transport (ESCRT) complex with soluble N-ethylmaleimide-sensitive factor attachment protein receptor (SNARE) proteins and their effectors, such as RAB GTPases. Ubiquitinated cargoes are recognized and sorted by the hepatocyte growth factor-regulated tyrosine kinase substrate (Hrs) of ESCRT-0. Phosphatidylinositol-3-phosphate (PI3P) promotes cargo organization through Hrs interaction. Subsequently, ESCRT-0 recruits ESCRT-I by interacting with the ESCRT-subunit tumor susceptibility gene 101 (Tsg101). ESCRT-I, together with ESCRT-II, promotes endosomal inward budding around clusters of ubiquitinated proteins while ESCRT-III recruits the charged MVB protein (CHMP) that polymerizes as a coil around the neck of the budding ILV pouch. ALG-2 (apoptosis-linked gene 2)-interacting protein X (ALIX) is an accessory ESCRT protein, which binds ESCRT-III subunits and facilitates the budding and abscission process for ILV formation (Gurung et al., 2021).

Above all, the existence of a route (ESCRT-independent lipid-mediated) that involves complex lipid and other protein related pathways in Exo biogenesis have also been highlighted (Skryabin et al., 2020). In ESCRT-independent lipid-mediated pathway, complex lipids, such as ceramide, can self-associate to form raft-like structures that contribute to the initial membrane curvature for inward budding to form intraluminal vesicles (Trajkovicet al., 2008). Tetraspanins, which constitute a subset of highly conserved membrane integral proteins, play important roles in protein scaffolding and anchoring in cellular membranes. Among them, CD9, CD63 and CD81 are often used as Exo biomarkers and it is well reported that they may influence Exo biogenesis and composition (Perez-Hernandez et al., 2013). CD63 (LAMP-3) interacts with apolipoprotein E to regulate ILVs sorting and is one of the main proteins used in engineered Exo to facilitate increased loading of cargoes and reporters (Babelman et al., 2020). CD9 interacts with metalloproteinase CD10 to enhance exosomal loading of CD10 and CD81-enriched microdomains and to provide cargo sorting (Perez-Hernandez et al., 2013). ESCRT-independent lipid-mediated regulation of Exo biogenesis depends on cell type. ESCRT-dependent and ESCRT-independent lipid-mediated pathways co-exist in numerous biological processes.

1.7 *Internalization and exosome cargo release within target cells*

Exo travel across the extracellular environment where they interact with target cell. They are incorporated into early endosomes following the typical endosomal pathway and may be released again through recycling endosomes (O'Brien et al., 2022). Exo are integrated through three different mechanisms*: i*) membrane fusion, in which SNARE and RAB proteins are required; *ii*) receptor-ligand binding, through major histocompatibility complex (MHC)-peptide complexes and tumor necrosis factor α (TNFα) ligands; *iii)* internalization via endocytic pathways, in which clathrin-mediated endocytosis (CME), caveolin-dependent endocytosis (CDE), lipid raft endocytosis, macropinocytosis and phagocytosis contribute to Exo uptake (Lau et al., 2023). Each mechanism is regulated by molecular pathways and environmental factors, leading to changes in Exo amount and composition.

Cellular signature is conserved in the secreted Exo and acts as recognition motifs for uptake by recipient cells and tissues *in vitro* and *in vivo*. Although specific targeting to recipient cells is crucial to deliver Exo molecular content and exert its function (Horibe

et al., 2018), a non-specific uptake is shared by all cell types (Zech et al., 2012) and is mediated by the Exo surface composition.

As already emphasized, the intracellular fate of integrated Exo follows the typical endosomal pathway, which involves fusion with lysosomes and may result in degradation. It is well reported that Exo fuse with lysosomes with the aim to degrade the excess cargoes. Endoplasmic reticulum (ER) is a nucleation site for translation and may be a route for lysosomal escape enabling Exo cargo release as ER scanning after Exo sorting into the endosome trafficking circuit. This would be a route of choice for Exo carrying mRNAs and miRNAs to release their cargoes in ER for rapid translation and modulation of gene expression (Santos et al., 2018; Gurung et al., 2021). Another option to evade lysosomal degradation implies that Exo are routed to a specialized and surface-accessible CD81 positive and lysosomal-associated membrane protein (LAMP)-1 negative intracellular compartment contiguous with the plasma membrane, in a manner similar to human immunodeficiency virus (HIV-1) and other viruses. Commonly, Exo cargoes effortlessly bypass degradation, thus affecting Exo-mediated functional changes in recipient cells (Deng et al., 2019; Gurung et al., 2021; Ha et al., 2016). Of note, through their molecular content, Exo can trigger downstream signaling cascade, impacting target cell activities. Cargo molecular content consists of lipids, proteins and nucleic acids, such as DNA, mRNA and noncoding RNA species (Doyle et al., 2021; Mashouri et al., 2019). Packaging of RNA within the lipid bilayer membrane is thought to provide protection from RNase digestion once released into the extracellular environment. Alternatively, different RNA species can also be stably associated with ribonucleoproteins (RNPs), such as Argonaute 2 (AGO2), or high- and low-density lipoproteins (HDLs and LDLs) (Abels and Breakefield, 2016).

Using various techniques, including next-generation sequencing (NGS), an abundance of small RNAs have been characterized. MicroRNAs (miRNAs) are one of the most abundant RNA species in Exo and play crucial roles in multiple biological processes, such as exocytosis, hematopoiesis and angiogenesis and participate in Exo-mediated cell communication and modulation of gene expression (Zhang et al., 2019). Other exosomal noncoding RNA species include ribosomal RNA (rRNA), long non-coding RNA (lncRNA), transfer RNA (tRNA), small nuclear RNA (snRNA), small nucleolar RNA and p-element-induced wimpy testis (piwi)-interacting RNA, all of which impact biological processes, particularly influencing tumor development (Zhang et al., 2019;

Ge et al., 2020). Interestingly, circular RNAs are also enriched and stable in Exo (Abels and Breakefield, 2016).

Exo can induce molecular signaling within target cell by directly interacting with extracellular receptors, be captured by direct fusion with the plasma membrane or get internalized. Exo exhibit on their surface a number of surface transmembrane ligands that can directly bind the membrane receptors on the recipient cell and generate downstream signaling cascade to activate the target cells. This is a common route to mediate immunomodulatory and apoptotic functions. Exo can also fuse with the plasma membrane and release their content directly into the cytosol of target cells and the uptake process is rapid and temperature-sensitive (i.e., decreased by low temperature) (Gurung et al., 2021). The latter process is a common route to affect gene expression of the recipient cell through regulatory noncoding RNAs carried by Exo, as observed in dendritic and tumor cells. Low pH in the TME, resulting in higher rigidity and increased sphingomyelin, could facilitate exosome fusion, thus making it a likely route to be adopted by tumor cells (Parolini et al., 2009).

Exo give rise to a vesicle-mediated pathway that is employed by cells in order to convey their own functions to distant sites. Although the main mechanisms of Exo biology have been delineated, the regulation of these EVs remains to be fully clarified.

1.8 *Exosomes in cancer*

In the TME, tumor progression is orchestrated by an extensive network of tumor, nonimmune and immune cells. In this scenario, a central role appears to be played by Exo, which participate to the transfer of a broad spectrum of signaling molecules between all these cells. Indeed, it was reported that Exo can alter the expression of molecules of the extracellular matrix (ECM), stromal cells such as cancer -associated fibroblasts (CAFs), cancer stem cells (CSCs), mesenchymal stem cells (MSCs) and immune cells in the TME (Zhang et al., 2019). Exo can further impact tumorigenesis and metastasis by regulating the interaction between T lymphocytes, B lymphocytes, macrophages, NK cells and the TME.

Moreover, the signaling molecules delivered by Exo could activate or inhibit immune cells to affect tumor progression (Filipazzi et al., 2012). Particularly, immune cells and lymphoid components of the TME, such as B and T lymphocytes, NK cells and macrophages, can be activated or inhibited by growth factors and cytokines carried by

Exo, resulting in the modulation of immune responses and tumor progression (Zou et al., 2021). Therefore, Exo may exert anti-tumoral or pro-tumoral activities depending on the tumor type, the TME features, the physiological conditions of the producing cell and the molecular content that Exo carry. Tumor cells may use an indirect and vesicle-based mechanism to affect either tumor growth or immune cell surveillance while complex lipids can influence Exo targeting in TME (Boussadia et al., 2021; Zech et al., 2012). Both colorectal and prostate cancer-derived Exo induce T cell apoptosis by carrying Fas ligand (FasL) (Abusamra et al., 2005; Huber et al., 2005). Treg -derived exosomal miRNAs, including miR-150-5p and miR-142-3p, can be delivered to DCs, prompting those DCs to produce more IL-10 and decreasing IL-6 upon lipopolysaccharide stimulation. In this context, these exosomes inhibit immune cell activities in tissues (Tung et al., 2018). Tumor associated macrophage (TAM)-derived Exo can deliver hypoxia inducible factor (HIF)-1α-stabilizing lncRNA which enhances the aerobic glycolysis and apoptotic resistance of breast cancer cells, while TAM-derived exosomal miR-365 significantly decreases the sensitivity of pancreatic ductal adenocarcinoma (PDAC) cells to gemcitabine supplying triphosphonucleotide pool and enhancing the activity of enzyme cytidine deaminase in PDAC cells (Chen et al., 2019; Binenbaum et al., 2018). M2 macrophage-derived exosomal miR-21-5p and miR-155-5p enhance colorectal cancer cell mobility, migration, and invasion (Lan et al., 2018).

On the other hand, a number of anti-tumoral Exo-triggered activities have been described. Lung carcinoma cell-derived Exo targeted the expression of CD107a in NK cells and produced immunosuppression through exosomal miR-23a (Berchem et al., 2016). Intestinal epithelial cell-derived Exo target T cells through the functional molecules MHC class I and II. These exosomal MHC complexes activate T cells by enhancing antigen presentation of DCs (Mallegol et al., 2007). CT26 mouse colon carcinoma cell and B16-F1 mouse melanoma cell-derived heat shock protein (HSP) 70-enriched Exo induce Th1 immune responses, resulting in the elimination of cancer cells *in vivo* (Cho et al., 2009). Chronic B lymphocytic leukemia-derived Exo transport glycoprotein (gp) 350 which binds to the CD154 receptor on B cells, rendering these cells immunogenic (Ruiss et al., 2011). Umbilical cord blood-derived Exo expressing tumor antigens such as MHC-I, MHC-II and tetraspanins (CD34, CD80) stimulate T cell proliferation to produce antitumor activity (Guan et al., 2014). Ligands, including TNFα, FasL and TNFα related apoptosis inducing ligand (TRAIL) expressed on Exo surface released by DCs can bind to TNFα receptors on tumor cells and trigger caspase

activation for apoptosis (Gurung et al., 2021). B-cell -derived Exo deliver MiR-330-3p that has been identified as a key factor in tumor progression. It downregulates TPX2 resulting in inhibition of melanoma cell proliferation (Xiong et al., 2023; Yao et al., 2018). NK cells that were previously exposed to neuroblastoma (NB) can secrete Exo containing NK cell receptors, such as CD56, NKG2D and KIR2DL2. These Exo can subsequently educate normal NK cells, providing increased cytotoxicity against NB tumor cells. Furthermore, NK cell-derived exosomal miR-186 promotes cytotoxicity against NB by directly targeting MYC-N, AURKA, TGFβ receptor (R) 1 and TGFβR2 (Yan et al., 2020).

Exo give rise to a considerable interest for clinical application as diagnostic biomarkers and therapeutic cargo carriers. A lower immunogenicity due to their biocompatibility and a bi-layered lipid structure, which protects the genetic cargo from degradation, makes them attractive as therapeutic. Another important aspect concerns the nanodimensions and membrane composition, which allow Exo to cross major biological membranes including the blood brain barrier. At present, the implementation of engineered Exo constitutes an active field in disease research, which fosters assessment of various therapeutic cargoes, enhancement of target selectivity and optimization of manufacturing (Zhang et al., 2019; Bunggulawa et al., 2018; Haney et al., 2015; Gurung et al., 2021). The cell-specific proteins and genetic materials contained in Exo could be explored as preclinical biomarkers in many types of cancers, such as lung cancer, hepatocellular carcinoma, pancreatic cancer, colorectal cancer, melanoma, breast cancer, prostate cancer, ovarian cancer, glioblastoma and nasopharyngeal carcinoma. Additionally, alternative therapeutic strategies, such as the inhibition of Exo secretion, the blockage of the uptake of Exo to specific receptors, or their tailor-made engineering have been proposed as novel approaches in cancer interventions (Zhou et al., 2021).

2. AIM OF THE STUDY

Eosinophils are important components of the TME where they play diverse roles depending on the type of cancer and on the environmental stimuli capable of shaping their phenotype and functions. IL-33 is a potent activator for eosinophils. IL-33 is expressed in several human cancers and can attract eosinophils directly via the ST2 receptor or indirectly through the activation of ILC2 and mast cells that in turn produce IL-5 and chemokines CCL5 and CCL24/eotaxin-2 released by tumor cells (Varricchi et al., 2017). Our previous studies demonstrated that mouse eosinophils activated with IL-33 acquire anticancer properties through the formation of eosinophil-tumor cell synapses (Andreone et al., 2019) that result in degranulation and tumor cell killing. As already reported in literature, eosinophils are able producers of exosomes through which they promote and autoregulate their functions (Cañas et al., 2017). Recent studies have highlighted that eosinophils from asthmatic subjects release greater quantities of exosomes, which produce several effects on lung structural cells, influencing the development and course of disease and airway remodeling (Cañas et al., 2018). Since extracellular vesicles, and particularly exosomes, play a major role in the TME and in anti-cancer responses (Cho et al., 2018; Filipazzi et al., 2012; Guan et al., 2014), in the present study we aimed to investigate the involvement of extracellular vesicle-mediated pathway deployed by IL-33 activated eosinophils for their anticancer activities. For this purpose, we employed mouse and human eosinophils stimulated with either IL-5 (Eo5) or IL-33 (Eo33) and confronted their capacity to reprogram tumor cell phenotype through the release of exosomes. We evaluated the impact of IL-33 on the quantity of exosomes released by eosinophils and their subsequent incorporation into target human and mouse tumor cells, as a mechanism to modulate gene expression and to subsequently induce functional variations (Deatherage et al., 2012; Doyle et al., 2019). We analyzed whether exosomes released by eosinophils following activation with IL-33 affected the expression of genes involved in tumor progression and in turn able to shape tumor cell phenotype. To do this, we focused on the study of several biological processes leading to cancer progression, such as cell cycle, proliferation, epithelial to mesenchymal transition and migration in mouse melanoma, fibrosarcoma, adenocarcinoma and in human melanoma models. Finally, we carried out bulk RNA sequencing (RNA-seq) of Eo5 and Eo33-derived exosomes in order to identify the molecules that could be involved in the regulation of the examined biological processes.

The results obtained in this project will provide further details on the role of exosomes in the tumor-immune crosstalk and their involvement in anti-tumor mechanisms which might affect tumor progression. Our findings will provide novel insights on the exosome-mediated potential of eosinophils within the TME and may open perspectives for possible exosome-based therapeutic options against cancer.

3. MATERIALS AND METHODS

3.1 *Tumor cell lines*

Murine B16.F10 metastatic melanoma cells (ATCC, CRL-6475), TC1 lung adenocarcinoma cells (provided by Dr. Guido Kroemer, Gustave Roussy Cancer Institute, France), MCA205 fibrosarcoma cells (Merk Millipore, SCC173) and human metastatic melanoma A375P cells (ATCC, CRL-3224) were employed. B16.F10 and A375P were cultured in DMEM High Glucose (EuroClone), while MCA205 in RPMI 1640 (EuroClone) both supplemented with 10% FBS, 1% glutamine, 1% penicillin streptomycin fungizone (PSF). TC1 were cultured in supplemented RPMI 1640 by adding 1% sodium pyruvate, 1% Hepes and 1% NEAA. All cell lines were constantly tested for morphology, absence of mycoplasma and passaged for no more than 3-4 times from thawing.

3.2 *Generation of bone marrow -derived eosinophils*

Bone marrow (BM) -derived murine eosinophils (mEo) were obtained following a differentiation protocol already described (Andreone et al., 2019) starting from BM cells from naïve C57Bl/6 mice. BM cells were extracted from both tibia and femur and treated with ACK lysis buffer (140 mM NH4Cl, 17 mM Tris HCl, pH 7.2) to discard erytrocites. Cells were plated at $2x10^6$/mL in RPMI 1640 containing 20% FBS, 1% glutamine, 1% PSF, 25 mM Hepes, 1X NEAA, 1 mM sodium pyruvate, supplemented with 100 ng/mL rmSCF (Cell Guidance Systems) and 100 ng/mL rmFLT3-L (Cell Guidance Systems) and cultured at 37 °C in 5% CO_2. On day 4, 10 ng/mL rmIL-5 (Peprotech) were added directly to the culture media. On day 8, cells were harvested, counted and splitted ($2x10^6$/mL) in two new T75 flasks containing fresh medium supplemented with 10 ng/mL rmIL-5. On days 10 and 12, 5 mL of fresh medium containing 10 ng/mL rmIL-5 were added. On day 14, cells were harvested, counted and replated $2x10^6$/mL in a new flask containing fresh medium and supplemented with 10 ng/ml rmIL-5 to generate a population of IL-5 eosinophils (mEo5) or with 100 ng/ml rmIL-33 (Biolegend) to generate a population of IL-33 eosinophils (mEo33). Cells are used on day 15 or 16, after overnight incubation with 10 ng/ml rmGM-CSF (MiltenyiBiotec), directly added in the culture media. At the end of differentiation,

eosinophil purity (>80%) was tested by flow cytometry ($CD11b^+$, $Siglec\text{-}F^+$, $Ly6G^-$ and $CD11c^-$) and/or cytospin.

3.3 *Isolation of human eosinophils*

Human eosinophils (hEo) were isolated starting from peripheral whole blood of healthy donors. Blood was stratified by dextran gradient (Dextran 70 BioChemica A1847, PanReac Applichem) to discard red blood cells. Once leukocytes have been collected from the higher phase, they were stratified by the use of the commercially Lymphosep, Lymphocyte Separation Media (Aurogene) to obtain, following 1800 rpm at room temperature for 20 minutes centrifugation without brake, the granulocyte pellet. Cells were treated with ACK lysis buffer to discard the survived erytrocites to the previous stages of separation. hEo were selected from the fraction of total granulocytes through negative immunomagnetic selection by the use of the commercially available Human Eosinophil Isolation Kit (Miltenyi Biotec). Highly pure hEo were obtained by depletion of the magnetically labeled $CD16^+$ cells. hEo purity (>86%) was tested by flow cytometry ($Siglec\text{-}8^+$, $CD3^-$ and $CD16^-$). Once the purity of hEo was assured, cells were plated $2x10^6$/mL in RPMI 1640 containing 1% glutamine, 1% PSF, 20% FBS, 25 mM Hepes, 1X NEAA, 1 mM sodium pyruvate, stimulated with 10 ng/mL rhIL-5 (Cell Guidance Systems) or with 50 ng/mL rhIL-33 (Prospec-Tany Technogene Ltd.) to generate a population of IL-5 -stimulated hEo (hEo5) or IL-33 -activated hEo (hEo33), respectively. Cells were placed in a 37 ◦C, 5% CO_2 incubator.

3.4 *Isolation of exosomes from mouse and human eosinophils*

For isolation of exosomes from mouse eosinophils, supernatants of mEo5 (Sup mEo5) and supernatants of mEo33 (Sup mEo33) at day 16 were subjected to centrifugations (1400 rpm 10 minutes at 4°C, then 3500 rpm 20 minutes 4°C) to remove intact cells and debris. Subsequently, Sup mEo5 and Sup mEo33 were subjected to serial ultra-centrifugations: 10000 x g 20 minutes at 4°C to remove granules and larger extracellular vesicles followed by 100000 x g 2 hours at 4°C to collect the resulting pellet of mEo5 and mEo33-derived exosomes (mExo5 and mExo33, respectively) (Coscia et al. 2016). For isolation of exosomes from human eosinophils, supernatants of hEo5 (Sup hEo5) and supernatants of hEo33 (Sup hEo33) were harvested, centrifuged 1400 rpm 10

minutes 4°C to remove cells and debris. Exo were purified by employing the Cell Culture Media Exosome Purification KIT (Norgen Bioteck Corp.) to obtain hEo5 and hEo33-derived exosomes (hExo5 and hExo33). Once isolated, all exosome preparations were resuspended in PBS or fresh medium depending on experimental requirements.

3.5 *Transmission electron microscopy*

mEo5 and mEo33 were fixed in 2.5% glutaraldehyde in 0.1 M cacodylate buffer, pH 7.4. Following washes in cacodylate buffer, cells were post-fixed in 1% OsO4 in the same buffer and further washed with 0.1 M cacodylate. Cells were then dehydrated in ethanol gradient from 50% to 100% (v/v) and embedded in Agar 100 resin (Agar Scientific) at 65 ◦C for 48 h. Ultrathin sections were obtained using an ultra-microtome and collected on 200-mesh grids, counterstained with uranyl acetate for 10 min and lead citrate for further 10 min. Samples were observed in a Philips 208s transmission electron microscope at 100 kW (Philips).

3.6 *Western blot*

Western blot analysis was performed according to standard procedures. Mouse and human Exo5, Exo33, and their Eo5 and Eo33 producing cells, were resuspended in sample buffer with freshly added 50 μM DTT. Mononoclonal antibodies (mAb) listed below were used in accordance to the manufacturer's instructions: mouse anti-Alix mAb (3A9 #MA183977, Thermo Scientific); mouse anti-TSG101 mAb (4A10 #GTX70255, GeneTex); human anti-CD81 mAb (1D6 #BTMC a-184 7T, Clinisciences). Protein concentrations were measured with BCA Protein Assay (Thermo Fisher Scientific). Eight μg of each sample were loaded in 10% gel (SureCast Acrylamide Solution (40%), Invitrogen), and transferred to nitrocellulose membrane (Amersham). The acquisition of the images and the quantifications analyses were achieved using FluorChem (Protein Simple). Bands were quantified by densitometry using ImageJ software.

3.7 *Generation and quantification of metabolically labeled fluorescent mouse or human exosomes by BODIPY FL C16labeling*

To quantify the number of secreted Exo from the producing mouse and human Eo, we generated fluorescent extracellular vesicles by labeling eosinophils with BODIPYFL C16 (4,4-difluoro5,7-dimethyl-4-bora-3a,4a-diaza-s-indacene-3-hexadecanoic acid) (C16) (Thermo Fisher), a fatty acid analogue that enters the cellular lipid metabolic pathway without affecting the natural lipid metabolism and homeostasis inside the cell. C16 rapidly integrates into major phospholipid classes producing green fluorescent Exo as a direct result of biogenesis (Coscia et al., 2016). Murine and human Eo5 and Eo33 were seeded $1x10^6$/mL in a 0,3% FBS RPMI 1640 cell-labeling medium containing 7 μM C16 and were incubated for 5 hours at 37°C in 5% CO_2. Cells were then washed and seeded at $1x10^6$ cell/mL in presence or absence of $0.05x10^6$/mL melanoma cells (mouse setting). Following 24 h incubation, $C16^+$ Exo-containing culture supernatants (ECSs) were harvested and ultra-centrifuged at 10000 × g, 4 °C to remove granules and larger extracellular vesicles. Subsequently, 1 mL aliquots (diluted 1:100) of fluorescent $C16^+$ Eo5 or $C16^+$ Eo33 ECS were analysed and enumerated through flow cytometry, by employing CytoFlex (Beckman Coulter) and analysed with the CytExpert Analysis Software (Beckman Coulter).

3.8 *Exosome uptake by target tumor cells*

The transfer of secreted $C16^+$ Exo5 and $C16^+$ Exo33 within tumor cells was evaluated using 0.4 μm pore-sized cell culture inserts (Corning Costar Corporation) that allow the transit of EVs but not of cells. Mouse and human Eo5 and Eo33 were labeled with C16, as described above. Mouse tumor cells (B16.F10, TC1, MCA205) were seeded ($2x10^5$ in 600 μL) in the bottom compartment of the 24-well plate while mouse $C16^+$ Eo5 and $C16^+$ Eo33 were plated ($2x10^6$ cells in 100 μl) in the upper insert (Eo:Tumor cells 10:1 ratio). Human A375P cells were seeded ($1x10^5$ in 600 μl) in the bottom compartment while human $C16^+$ Eo5 and $C16^+$ Eo33 ($1x10^6$ in 100 μl) were placed in the topside of the transwell (Eo:Tumor cells 10:1 ratio). Controls consisted of tumor cells cultured alone, in the absence of eosinophils. After 2 to 18 h incubation at 37°C in 5% CO_2, tumor cells were harvested and analysed by flow cytometry for acquisition of green fluorescence, indicative of $C16^+$ Exo transfer to target tumor cells.

3.9 *Culture of tumor cells with eosinophils, eosinophil supernatants and eosinophil -derived exosomes*

For co-culture of Eo5 and Eo33 with tumor cells, mouse B16.F10, TC1 or MCA205 and human A375P were cultured alone or with, respectively, mouse or human Eo5 or Eo33 at an Eo:tumor cells 4:1 ratio. Co-cultures were placed at 37°C and 5% CO_2 incubator. The following day, culture supernatants were collected, centrifuged 1400 rpm, 10 minutes, 4°C and stored for further analyses. Eosinophils were removed by extensive washes with PBS and adherent tumor cells were harvested and employed for flow cytometry and gene expression analyses.

In some experiments, tumor cells were directly exposed and overnight incubated with Sup Eo5 and Sup Eo33 or with tumor cells plus Eo5 or Eo33 co-culture supernatants. At the end of overnight incubation, tumor cells were washed with PBS once, harvested and employed for molecular studies.

To evaluate the Eo Exo -mediated activities on tumor cells, preparations of human or mouse Exo5 and Exo33 were administered to the tumor cell culture: 20-40 $x10^6$ mExo5 or mExo33 per well, 40-80 $x10^6$ hExo5 or hExo33 per well that corresponds to Exo amount contained in each mL of the deriving ECS in which Eo were initially plated $2x10^6$ cells/mL. Tumor cells were cultured with Exo overnight at 37°C in 5% CO_2 and subsequently harvested and employed for flow cytometry and molecular analyses.

3.10 *Cell proliferation assays*

To test the capacity of eosinophils in inhibiting melanoma cell proliferation, $1x10^5$ A375P were co-cultured, as described, with $3x10^5$ hEo5 or hEo33 in 6-well plates for 24 hours (Eo:Tumor cells 3:1 ratio). Following incubation, hEo5 and hEo33 were washed out with PBS and the remaining adherent tumor cells were fixed with methanol, stained with 0,1% Crystal Violet (in a 20% ethanol solution). A number of images of Crystal Violet stained tumor cells were captured by using an EVOS-FL fluorescence microscope (Life Technologies) and quantitative analysis of the tumor cell covered area was performed with ImageJ Software. To test the anti-proliferative capacity of eosinophil-derived exosomes, an MTS assay was carried out by plating one thousand tumor cells in 200 µL of fresh medium in flat 96-well plates (Corning Inc.). Once tumor cells have adhered, mExo5 or mExo33 were added to the tumor cell culture as described above and incubated up to 120 h. At the end of each incubation, 20 µL per well of 3-

(4,5-dimethylthiazol-2-yl)-5-(3-carboxymethoxyphenyl)-2-(4-sulfophenyl)-2H-tetrazolium (MTS) (Promega CellTiter 96™ AQ_{ueous} Nonradioactive Cell Proliferation Assay Kit, Thermo Fisher Scientific) were added and incubated for 1 hour at 37°C in 5% CO_2. Absorbance was measured in a spectrophotometer at a wavelength of 490 nm.

3.11 *Annexin V apoptosis assay*

Mouse B16.F10 melanoma cells were labeled with PKH26 Red fluorescent Cell Linker (Sigma) and were plated $5x10^4$ per well in 100 µL of fresh medium in round bottomed 96-well plates (Corning Inc.). mEo5 and mEo33 were either untreated or pre-treated, respectively, with 2 µM and 8µM GW4869 (N,N'-Bis[4-(4,5-dihydro-1H-imidazol-2-yl)phenyl]-3,3'-p-phenylene-bis-acrylamide dihydrochloride) (Sigma), an inhibitor of exosome biogenesis/release, by incubation for 4 hours at 37°C in 5% CO_2. Eo were washed with PBS and resuspended at $2,5x10^6$ per 100 µL and co-cultured with B16.F10 (Eo:Tumor cells 50:1 ratio) for 5 hours at 37°C in 5% CO_2. Tumor cells were then stained with Annexin-V (e-Bioscience, Thermo Fisher Scientific) and then analyzed by flow cytometry. Apoptosis of target tumor cells was calculated as the percentage of Annexin-V^+ cells among gated $PKH26^+$ population.

3.12 *Tumor spheroid formation*

Multicellular tumor spheroids from murine B16.F10 melanoma, MCA205 fibrosarcoma, TC1 adenocarcinoma and human A375P melanoma cells were generated in flat ultralow-attachment surface 96-well plates (Corning Inc.). Five hundred cells were cultured in 200 µL of fresh medium, 200 µL of supernatants (diluted 1:2) or in in 200 µL of fresh medium in which were added purified exosomes.
Visible photomicrographs were generated at various times (from the fourth to the sixth day) by using an EVOS-FL fluorescence microscope (Life Technologies).

3.13 *Cell cycle assay*

Mouse B16.F10 melanoma, TC1 lung adenocarcinoma and human A375 melanoma cells were plated in 6-well plates and incubated for 24 hours and 48 hours with the corresponding mouse and human Exo5 or Exo33. At the end of each incubation, tumor cells were harvested, washed with PBS and resuspended in PBS, 0,1% Glucose. Tumor

cells were fixed in 1 mL of ice-cold 70% ethanol. One day later, samples were centrifuged 1000 rpm, 10 minutes, 4°C and pellets were stained with 0,5 mL of the commercially available FxCycle™ PI/RNase Staining Solution (Thermo Fisher Scientific). Samples were incubated for 15–30 minutes at room temperature, protected from light, and then run on a Gallios flow cytometer (Beckman Coulter). DNA content was measured using fluorescent PI DNA stains that exhibit emission signals proportional to DNA mass. Analysis was performed by using the Kaluza Analysis Software (Beckman Coulter).

3.14 *Wound healing scratch assay*

For migration tests, $5x10^5$ B16.F10 cells were plated in 6-well plates and exposed overnight to mExo5 or mExo33. Confluent cells were scratched using a 200 μL sterile tip and then incubated at 37°C in 5%CO_2. Images were captured at various time points by using EVOS-FL fluorescence microscope. Captured images were analysed using ImageJ software.

3.15 *mAbs and flow cytometry*

Mouse eosinophils were characterized with the following fluorescently labeled mAbs: APC anti-CD11b (clone M1/70), BV421 anti-Siglec-F (clone E50-2440; BD Biosciences), FITC anti-Ly6G (clone1A8; Biolegend) and PE anti-CD11c (clone N418; Biolegend). Human eosinophils were characterized with the following fluorescently labeled mAbs: PE-Vio770 anti-Siglec-8 (clone 7C9; Miltenyi Biotec), FITC anti-CD16 (clone REA423; Miltenyi Biotec) and anti-CD3 (clone OKT3; Biolegend). For the investigation of E-Cadherin expression on tumor cells, mouse tumor cells (B16.F10 and TC-1) were labeled with PKH26 Red fluorescent Cell Linker (Sigma) prior to co-culture with mEo5 or mEo33 and then stained with fluorescent anti-mouse/human CD324 (clone DECMA-1; Biolegend).

3.16 *Real time qPCR*

Total RNA was extracted from tumor cells by using TRIsure reagent (Bioline). mRNA was reverse transcribed by means of Tetro cDNA Synthesis Kit (Bioline). Quantitative real time PCR (qPCR) with forward and reverse primers (Eurofins Genomics) was

performed using Sensimix Plus SYBR Kit containing the fluorescent dye SYBR Green (Bioline) and by means of an ABI 7500 Real-time PCR system (Applied Biosystems, Thermo Fisher Scientific). The conditions of real time qPCR reaction were given as follows: 15 seconds at 95°C, 30 seconds at 60°C and 45 seconds at 72° for 40 cycles. Triplicates were performed for each experimental point. Quality and specificity of amplicons in each sample were detected by dissociation curve analysis. For quantization, threshold cycle (CT) values were determined by the sequence detection system software (Applied Biosystems). Data were normalized to HPRT housekeeping gene (2-ΔCt method).

3.17 *RNA sequencing of IL-5 and IL-33 stimulated eosinophils and derived exosomes*

RNA Sequencing (RNA-Seq) was performed in collaboration with the Immunology Unit of University of Palermo. RNA was extracted from mEo5 and mEo33 and from mExo5 (~3 x 10^8) and mExo33 (~ 6 x 10^8) isolated from their respective culture medium (day 16 of differentiation) by serial ultracentrifugations as described above. Two experimental replicates for each sample (mEo5, mEo33, mExo5 and mExo33) were prepared. Quality and quantity of extracted RNA from each sample were measured by the use of the spectrophotometer NanoDrop 1000 (Myco Instumentation). For the library preparation, the kit SQK-PBK004 (Nanopore Technologies) was employed. To amplify all types of RNA molecules present in the samples, 1 µg or 280 ng of total RNA extracted from eosinophils or their corresponding Exo, respectively, were reverse transcribed into cDNA using the LunaScript RT SuperMix Master Mix (NEB), following the manufacturer's protocol. This master mix contains random hexamer and poly-dT primers, ensuring even coverage across the length of the RNA targets. Subsequently, the reverse transcribed samples were purified using AmpureXP beads (Beckman Coulter), following the manufacturer's instructions, and eluted in 49 µl of nuclease-free water. To determine the amount of cDNA present in each sample, Bioanalyzer 2100 (Agilent) was used with the Agilent High Sensitivity DNA Kit (Agilent). The library for sequencing was prepared according to the SQK-PBK004 protocol version PBK_9073_v1_revR_14August2019, starting from the End-prep step. Since the samples did not reach the suggested 100 femto-moles by the Nanopore protocol for library preparation, the entire volume (48 µl) was mixed with 3.5 µl of

Ultra II End-prep reaction buffer and 3 µl of Ultra II End-prep enzyme mix (NEB), resulting in a final volume of 54.5 µl. Next, to increase the concentration and to add a unique barcode sequence to each sample, an adapter ligation step was followed by an amplification step using barcoded primers and the enzymes and Thermal Profile recommended in the protocol. After amplification, each library was purified using AmpureXP beads, and, to determine the library molarity, the samples were analyzed on the Bioanalyzer 2100 using the DNA 12000 kit, following the manufacturer's instructions. Subsequently, the libraries were pooled into a total of 50 femto-moles in 10 µl of 10 mM Tris-HCl pH 8.0 with 50 mM NaCl. This pooled library was loaded onto the MinION Mk1B (Oxford Nanopore, cat no MIN-101B) flow cell after the adapter ligation step. The MinION sequencer was connected to a PC, and MinKNOW software version 22.12.7 was used to sequence the libraries and perform base-calling of the generated reads, resulting in fast5 and fastq files, respectively. The produced fastq files were sent to IFOM/Cogentech SRL company service for Bioinformatic analysis. Fastq files were processed bynfcore/nanoseq pipeline (https://nf-co.re/nanoseq) by using the Ensemble version 109 for both fasta (ftp://ftp.ensembl.org/pub/release-109/fasta/mus_musculus/dna/Mus_musculus.GRCm39.dna.primary_assembly.fa) and gft(ftp://ftp.ensembl.org/pub/release109/gtf/mus_musculus/Mus_musculus.GRCm39.109.gtf) files. The following parameters were employed: input sample_sheet, protocol cDNA, skip_demultiplexing, skip_fusion_analysis, skip_differential_analysis. Pipeline was used for quality control, alignment, quality control of alignment, reconstruction and quantification of genes and transcripts. FeatureCount and StringTie tools were used for transcript quantification. DexSeq (|log2FC|>0.58) was employed for the differential analysis. For normalization, Upper Quartile Normalization was employed. The data fields are subdivided in metadata, grouping data and numeric data (reads and computations, Table I), all associated to mEo and mExo information. This Excel dataset file was used as staring dataset for bioinformatic analysis to identify key genes and to display Volcano plot on mExo5 and mExo33 genes. Computed data were yielded by specific *ad hoc* formula (Excel notation) extended to the whole data column (Table II). The estimate of differential expression was calculated as log2 values of the Normalized gene reads (log2(NormCount+1) in the two sample groups and were reported in "Dataset.xlsx" Excel file (n=149223 genes). Bioinformatics workflow for the differential analysis of the normalized RNA-seq data were performed on the basis of the

data in "Dataset.xlsx". Specifically, several metadata and grouping data fields were available for both mEo and mExo reads (Table I and II).

Table I. Structure of the Excel dataset used to identify key exosomes mRNAs. *Green text, Eosinophils data; Red text, Exosome data.*

Field label name*	Data class	Data type	Field use
transcript_id gene_id Chr Start End Strand gene_name	Metadata (alphanumeric)	Alphanumeric	Gene identification
gene_biotype transcript_biotype gene_source transcript_source gft_source transcript_support_level	Grouping data	Alphanumeric	Gene categorization and filtering
EO_5_R1 EO_5_R2 EO_33_R1 EO_33_R2	Experimental data	Numeric, normalized data associated to eosinophils reads	Analysis* and filtering
EO_5_R1_2^n EO5_R2_2^n EO33_R1_2^n EO33_R2_2^n EO33vsEO5_FC1 EO33vsEO5_FC2 EO33vsEO5_FC3 EO33vsEO5_FC4 EO33vsEO5_FC-AVG log2(EO33vsEO5-FC-AVG) minus_log10(pvalueEO)	Experimental data	Numeric, computed data (eosinophil data)	Analysis*, filtering and Volcano plot data extrapolation
EXO_5_R1 EXO_5_R2 EXO_33_R1 EXO_33_R2	Experimental data	Numeric, normalized data associated to exosome reads.	Analysis* and filtering
EXO_5_R1_2^n EXO5_R2_2^n EXO33_R1_2^n EXO33_R2_2^n EXO33vsEXO5_FC1 EXO33vsEXO5_FC2 EXO33vsEXO5_FC3 EXO33vsEXO5_FC4 EXO33vsEXO5_FC-AVG log2(EXO33vsEXO5-FC-AVG) minus_log10(pvalueEXO)	Experimental data	Numeric, computed data (exosome data)	Analysis*, filtering and Volcano plot data extrapolation

* R1, R2, FC1, FC2, FC3, FC4 acronyms delineate replicates of the same experimental condition. Eo and Exo acronyms delineate the eosinophil and exosome data, respectively.

Table II. Employed formula per numeric normalized experimental data. *Green text, eosinophils; red text, exosomes.*

Field label name*	Formula used for computations	Field usage
EO_5_R1 EO_5_R2 EO_33_R1 EO_33_R2	None. Eosinophil reads provided as $\log_2$(normalized counts – 1).	Source read data; filter.
EO_5_R1_2^n EO5_R2_2^n EO33_R1_2^n EO33_R2_2^n	Exponential (base 2) values yielded by the EO_5_R1, EO_5_R2, EO_33_R1 and EO_33_R2 (eosinophils) data	Data for t test significance analysis between experimental conditions; filter.
EO33vsEO5_FC1 EO33vsEO5_FC2 EO33vsEO5_FC3 EO33vsEO5_FC4	Fold change values obtained by EO_33_2^n/EO_5_2^n ratios, (in combination) to yield 4 different FC ratios.	Data used to compute the Average fold change values.
EO33vsEO5_FC-AVG	Average value from the four eosinophil FC ratios.	Filter
Test t EO	Yields p values from T test between EO33 and EO5 replicate values.	Filter for significant vs non-significant EO genes
log2(EO33vsEO5-FC-AVG)	Base-2 logarithm from mean FC (eosinophils).	X Scale factor parameter for Volcano plot of genes with specific mean FCs
minus_log10(pvalueEO)	Inverse of the base-10 logarithm associated to each Test t EO value.	Y Scale factor parameter for Volcano plot for significantly expressed genes.
EXO_5_R1 EXO_5_R2 EXO_33_R1 EXO_33_R2	None. Exosome reads provided as $\log_2$(normalized counts – 1).	Source read data; filter.
EXO_5_R1_2^n EXO5_R2_2^n EXO33_R1_2^n EXO33_R2_2^n	Exponential (base 2) values yielded by the EXO_5_R1, EXO_5_R2, EXO_33_R1 and EXO_33_R2 data	Data for t test significance analysis between Experimental conditions; filter.
EXO33vsEXO5_FC1 EXO33vsEXO5_FC2 EXO33vsEXO5_FC3 EXO33vsEXO5_FC4	Exosome Fold change values obtained by EXO_33_2^n / EXO_5_2^n ratios, (in combination) to yield 4 different FC ratios.	Data used to compute the Average fold change values.
EXO33vsEXO5_FC-AVG	Average value from the four exosome FC ratios.	Filter
Test t EXO	Yields p values from T test between EXO33 and EXO5 replicate values.	Filter for significant vs non-significant EXO genes
log2(EO33vsEXO5-FC-AVG)	Base-2 logarithm from mean FC.	X Scale factor parameter for Volcano plot of genes with specific mean FCs
minus_log10(pvalueEXO)	Inverse of the base-10 logarithm associated to each EXO p-value from t test analysis.	Y Scale factor parameter for Volcano plot for significantly expressed genes.

* R1, R2, FC1, FC2, FC3, FC4 acronyms delineate replicates of the same experimental condition. Eo and Exo acronyms delineate the eosinophil and exosome data, respectively.

RNA sequencing process has successfully identified 149223 transcripts in our samples, including protein coding RNAs (mRNAs), miRNAs, long noncoding RNAs (lncRNAs), ribosomal RNAs (rRNAs), pseudogenes, small nuclear and small nucleolar (sn and snoRNAs), mitochondrial RNAs (mtRNAs) and other unprocessed transcripts. In order to exclusively select mRNAs from "Dataset.xlsx" file, we applied a sequential Excel filtering process on the "Gene-Biotype" and "protein coding" fields (Table I), resulting

in 101830 selected mRNAs. The base-2 logarithmic expression values were converted to exponential values to calculate all the computed data to be used for Volcano plot and extrapolation of significant genes, which will be distinguished based on *t*-test analysis on mEo and mExo data (exponential data, Table II). To cross-filter transcripts mainly expressed in exosomes (either mExo5 or mExo33), which simultaneously displayed a similar behavior in their producing cell (mEo5 or mEo33, respectively), we used the mean FC and p-values data fields, by excluding all genes with Eo and Exo FC values between 0.5 and 2 values. This cross-filtering process yielded transcripts whose expression is significantly higher in mExo33 with respect to mExo5 (mExo33 genes, n=22) and mRNAs whose expression is significantly higher in mExo5 compared to mExo33 (mExo5 genes, n=16). To represent the differential expression of mExo5 and mExo33 genes in Volcano plot, we generated an Excel dataset grouping the two cluster of genes and the resting (non-significant) transcripts (Table II). The graph was obtained by exploiting the VolcaNoseR2 R tool, an R script web-based tool (https://huygens.science.uva.nl/VolcaNoseR2/; Goedhart and Luijsterburg, 2020). Specifically, negative Log10 from mEo or mExo p-values (namely, -log10(p value), Table I and Table II) and Log2 mEo or mExo mean FC values were used to obtain a Volcano plot displaying the mExo5 and mExo33 genes. FC value threshold was set up between -1 and +1, while the significance threshold was configured on 1.1 (namely, around the 0.05 p raw value). The differential expression of these two clusters of genes was visually plotted as a heatmap graph by using Orange Data Mining software (https://orangedatamining.com/; Ramadhani et al., 2022). Heatmaps represent mExo5 and mExo33 hierarchically clustered genes (rows) and experimental conditions (column) to depict the similarity extent between the clustered factors. Finally, to evaluate the biological processes of the two mExo5 and mExo33 transcript clusters, we performed a Gene Ontology (GO) analysis through the Logically Accelerated Gene Ontology (LAGO) web-based tool (https://go.princeton.edu/cgi-bin/LAGO; Boyle et al., 2004). GO terms were considered significant at a 0.05 cut off value. GO Biological Process (BP) analysis was confirmed throw GO analysis on G-profiler database (https://biit.cs.ut.ee/gprofiler/gost; Kolberg et al., 2023) by running mExo5 and mExo33 as multiquery. The significance threshold was calculated as False Discovery Rate (FDR) upon a 0,05 value cut off.

3.18 *Statistical analysis*

Statistical analyses were performed using GraphPad Prism Software (GraphPad, La Jolla, CA). One-way ANOVA analysis of variance was performed to compare means among multiple groups, followed by post-hoc testing (Tukey). Values were considered significant when the probability was below the 5% confidence level ($p < 0.05$).

4. RESULTS

4.1 *Activation of human eosinophils with IL-33 promotes tumor cell killing*

Our previous studies suggested that mouse bone marrow-derived eosinophils terminally differentiated with IL-33 constitute a population of highly activated Eo (Lucarini et al., 2017). In fact, we demonstrated that activation with IL-33 leads to both adhesion of eosinophils to target tumor cells and convergence of lytic granules (containing cationic proteins EPX and ECP) to the Eo-tumor cell synapses, responsible for degranulation and subsequently tumor cell death through apoptosis (Andreone et al., 2019). Based on these premises, we extended these findings in the human setting. We isolated hEo from the peripheral blood of healthy volunteers by magnetic cell sorting. We characterized the phenotype of hEo population and flow cytometry analysis revealed that cell purity was higher than 86% (Siglec8^{+} CD16^{-} CD3^{-}) (Figure 1). We cultured hEo for 18 h in the presence of either IL-5 (hEo5) or IL-33 (hEo33) and then tested their cytotoxic activity against A375P human melanoma cells. Upon activation with IL-33, we observed that hEo promote human melanoma cell killing through a significant reduction of A375P cell-covered area after 24 hours co-culture, with respect to the condition in which A375P were co-cultured with hEo5 (Figure 2).

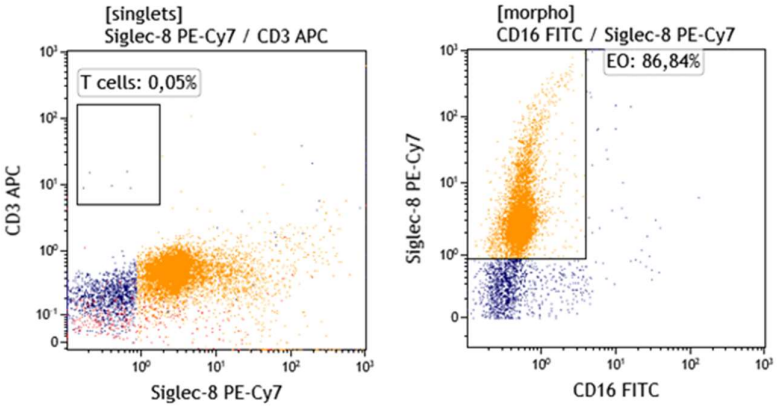

Figure 1. Flow cytometry analysis of purified human eosinophils. Magnetically sorted human blood-derived eosinophils were labelled with fluorescent mAb to detect Siglec-8, CD3 and CD16. Eosinophils were identified as Siglec-8+ CD3- CD16-.

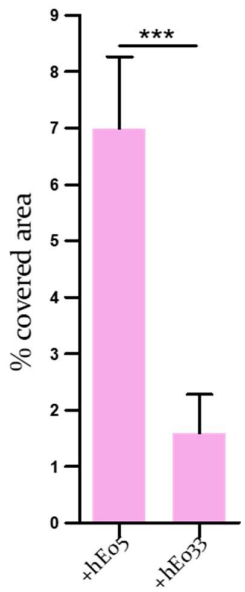

Figure 2. IL-33 activated human eosinophils exert cytotoxic activity against tumor cells. HEo5 and hEo33 were co-cultured with A375P human melanoma cells for 24 hours, then washed out and adherent tumor cells were stained with Crystal Violet. Quantitative analysis of the tumor cell covered area in the indicated culturing conditions is shown. Data are represented as fraction of area occupied by the indicated tumor cells with respect to the total field area. Mean values ±SD from 10 different microphotographs per condition are shown. *** $p < 0.001$.

4.2 *IL-33 activated eosinophils modulate the expression of genes involved in tumor progression in mouse and human tumor cells*

Since cytotoxicity does not occur in all cancer cells following co-culture with IL-33 activated Eo, we explored further effects on the surviving tumor cells. We therefore carried out gene expression analysis in mouse and human tumor cells after 24 h co-culture with mouse or human, respectively, Eo5 and Eo33, focusing on cell cycle inhibitor molecules that may result in cell cycle arrest and, therefore, a possible block of tumor cell proliferation.

Our qPCR results revealed that A375P melanoma cells co-cultured with hEo33, but not with hEo5, significantly up-regulated the expression of cyclin -dependent kinase (CDK) inhibitor 1a (*Cdkn1a)* and CDK inhibitor 1b (*Cdkn1b)* genes, whose role is inhibition of the G1/S transition and consequently cell cycle arrest (Hume et al., 2021; Figure 3a). Similarly, upon contact with mEo33, B16.F10 expressed higher levels of *Cdkn1a* (Figure 3b) while MCA205 show a substantial overexpression of *Cdkn1b* with respect to cells cultured alone or in the presence of mEo5 (Figure 3c).

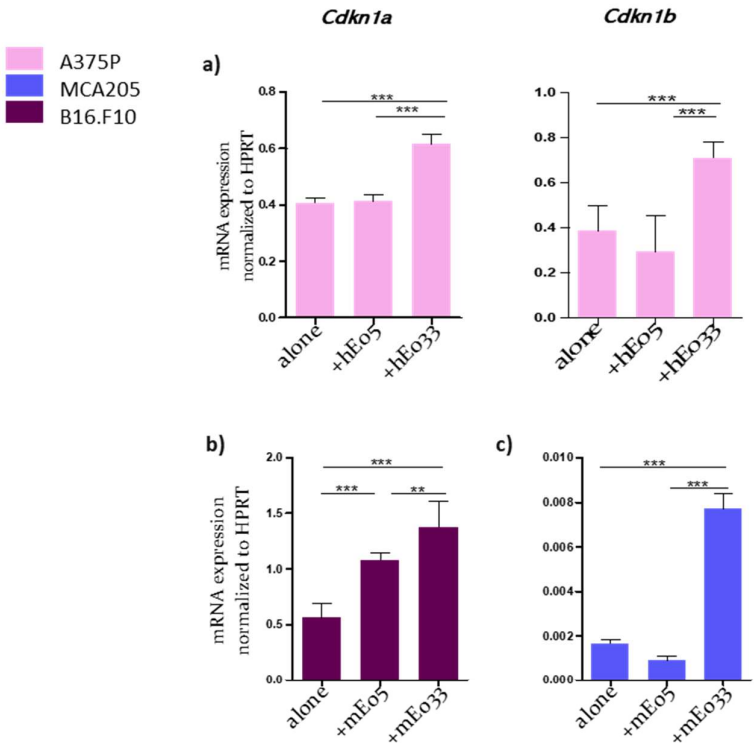

Figure 3. IL-33 activated eosinophils modulate the expression of genes involved in cell cycle blockade in mouse and human tumor cells. (a) Human melanoma (A375P), (b) murine melanoma (B16.F10) and (c) fibrosarcoma (MCA205) cells were co-cultured for 24 hours respectively with human and mouse Eo5, Eo33 or left alone. Eosinophils were washed out and adherent tumor cells were subjected to RNA extraction. The expression of *Cdkn1a* and *Cdkn1b* genes was analysed by qPCR. Mean values ±SD from triplicates and one representative experiment out of three are shown. ***P<0.0001. One Way Anova analysis of variance with Tukey's Multiple Comparison Test.

To further investigate phenotypic changes induced by Eo33 in tumor cells, we studied epithelial to mesenchymal transition (EMT) through the evaluation of the expression of the main markers that orchestrate this tumor progression -associated process, particularly E-Cadherin (related to epithelial and anti-tumoral features) and N-Cadherin (related to mesenchymal and pro-tumoral features) (Debnath et al., 2022). Through gene expression analysis, we found that B16.F10 (Figure 4a), MCA205 (Figure 4b) and TC1 (Figure 4c) significantly up-regulated the expression of *Cdh1,* that encodes for the epithelial marker E-Cadherin, while downregulated *Cdh2,* that encodes for N-Cadherin mesenchymal marker, following 24 h co-culture with mEo33, with respect to tumor cells cultured alone or with mEo5. In a similar fashion, A375P human melanoma cells up-regulated *Cdh1*, while expressed lower levels of *Cdh2*, after co-culture with hEo33, with respect to hEo5 or cultured alone (Figure 4d).

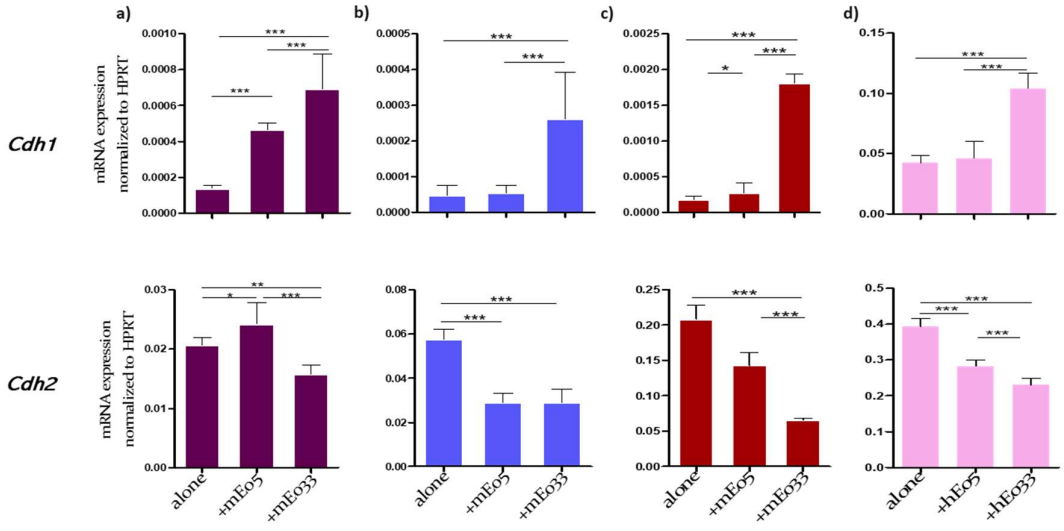

Figure 4. IL-33 activated eosinophils modulate the expression of genes involved in epithelial to mesenchymal transition in mouse and human tumor cells**.** Murine (a) B16.F10 melanoma, (b) MCA205 fibrosarcoma, (c) TC1 lung adenocarcinoma and human (d) A375P melanoma were co-cultured for 24 h respectively with mouse and human Eo5, Eo33 or left alone. Eosinophils were washed out and adherent tumor cells were subjected to RNA extraction. The expression of *Cdh1* and *Cdh2* genes was analysed by qPCR. Mean values ±SD from triplicates and one representative experiment out of three are shown. *P<0.01, **P<0.001, ***P<0.0001. One Way Anova analysis of variance with Tukey's Multiple Comparison Test. One representative experiment out of three is shown.

In addition, flow cytometry analysis of E-Cadherin membrane expression performed on B16.F10 and TC1 cells confirmed the increased levels of the epithelial marker upon 24 h tumor cell-mEo33 contact (Figure 5). Of note, up-regulation of E-Cadherin was observed even when tumor cells were cultured with mEo33 in 0.4 µm-pore sized transwell plates to avoid direct cell-cell contact (Figure 6). The ensemble of these observations indicates that besides the cytotoxic effects, IL-33 activated eosinophils may exert anticancer activities also through regulation of cell cycle and EMT process in tumor cells.

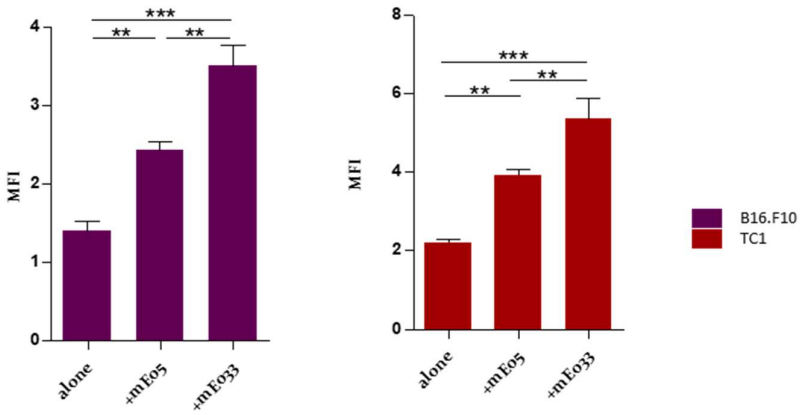

Figure 5. Flow cytometry analysis of E-Cadherin expression in mouse B16.F10 melanoma (violet) and TC1 lung adenocarcinoma (red) cells co-cultured with mEo5, mEo33 or left alone. Mean values ±SD from triplicates and one representative experiment out of two are shown. **P<0.001, ***P<0.0001. One Way Anova analysis of variance with Tukey's Multiple Comparison Test.

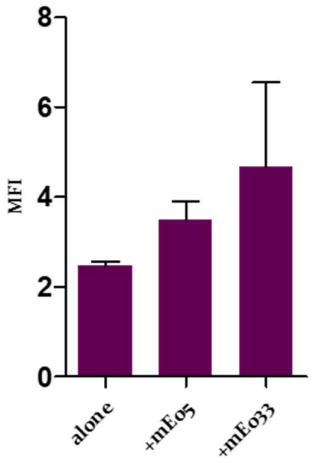

Figure 6. Flow cytometry analysis of E-Cadherin expression in mouse melanoma B16.F10 cells cultured alone or co-cultured with mEo5 or mEo33 in 0.4 μm-pore sized transwell plates to avoid direct cell-cell contact. Mean values ±SD from triplicates and one representative experiment out of two are shown.

4.3 *Activation of eosinophils with IL-33 increases exosome secretion*

The observation that direct cell-cell contact was not required for tumor E-Cadherin up-regulation by Eo33 prompted us to investigate the possible role of Exo in mediating Eo33 anti-tumor activities. Eosinophils are able to produce Exo, which mediate their biological functions (Cañas et al., 2021). We isolated Exo from mouse and human Eo5

and Eo33 culture supernatant and assessed the expression, by western blot analysis, of the often termed “exosomal marker proteins”, often enriched in the vesicles compared to the cell lysate (Doyle et al., 2019; Tauro et al., 2012; Morita et al., 2007). mExo5 and mExo33 expressed the exosomal markers Alix and Tsg101 (Figure 7a), while human eosinophil-derived exosomes, hExo5 and hExo33, expressed the exosomal marker CD81 (Figure 7b). Since the quantity of secreted Exo may vary depending on whether the producing cells are experiencing different stressors or stimuli (Kalluri et al., 2016), we enumerated exosomes released by human and mouse eosinophils following stimulation with either IL-5 or IL-33. To this end, we generated fluorescent mouse and human Exo by BODIPY FL C16 metabolic labelling of the producing eosinophils and quantified them by flow cytometry analysis (Figure 7c). The measurement of C16 - associated green fluorescence, indicative of $C16^{+}$ Exo secretion within the collected Sup Eo5 and Sup Eo33, revealed that both mouse and human Eo33 produced higher amounts of Exo (~ 2-fold) with respect to Eo5 (Figure 7d). We hypothesized that this result may correlate with the higher activation state of Eo33. Additionally, the presence of tumor cells further boosted mEo33-derived exosome secretion (Figure 8a). Furthermore, transmission electron microscopy (TEM) of mEo33 co-cultured with B16 melanoma cells, confirmed the typical ultrastructural organization of mEo and clearly showed mExo release from Eo33 secreting cell adjacent to tumor cells (Figure 8b). These observations demonstrate that IL-33 activated Eo release exosomes in the presence of tumor cells and suggest the possibility that these vesicles may influence the tumor once incorporated.

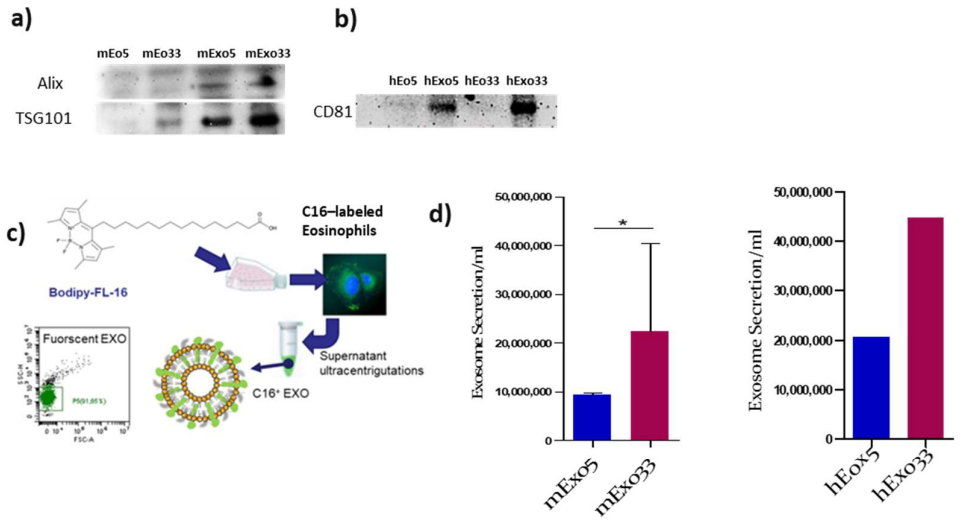

Figure 7. Analysis and quantification of mouse and human eosinophil-derived exosomes. Western blot analysis of exosomal markers in (a) mouse and (b) human Exo5 and Exo33. (c) Generation of fluorescent exosomes by metabolic labelling of eosinophils with Bodipy-C16 and (d) quantification of $C16^{+}$ mouse and human Exo5 and Exo33 by flow cytometry. Mean values ±SD from triplicates and one representative experiment out of two are shown. *P<0.01. Unpaired t-test.

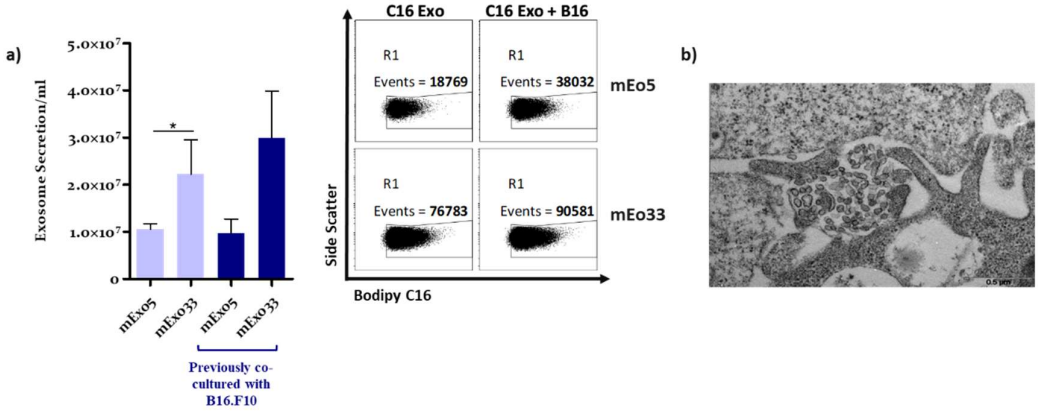

Figure 8. (a) Quantification by flow cytometry of $C16^{+}$ mExo5 and mExo33, from mEo5 and mEo33 cultured alone or in the presence of B16.F10 melanoma cells. Mean values ±SD from triplicates and one representative experiment out of two are shown. *P<0.01. Unpaired t-test. (b) Micrograph of transmission electron microscopy (TEM) of mEo33 co-cultured with B16.F10 that illustrates the secretion of exosomes in the vicinity of tumor cells. One representative micrograph is shown.

4.4 *IL-5 and IL-33 eosinophil -derived exosome uptake within target tumor cells*

In all cell types a non-specific Exo uptake is reportedly mediated by the surface composition of these vesicles (Zech et al., 2012). The Exo internalization process within the target cell is a necessary condition to determine their molecular and bioactive cargo release (Joshi et al., 2020; Tian et al., 2013). Based on this premise, we evaluated the internalization of $C16^+$ Eo-derived Exo within mouse and human tumor cells by co-culturing C16-labelled eosinophils and tumor cells "contactless" in 0.4 μm-pore sized chambers and by analyzing the transfer of fluorescent Exo into tumor cells by flow cytometry. We found that both $C16^+$ mExo5 and $C16^+$ mExo33 achieve 100% of internalization in B16.F10 (Figure 9a) and MCA205 (Figure 9b) cells after just 2 hours incubation with $C16^+$ mEo5 and $C16^+$ mEo33, while up to 60-70% of integration is observed into TC1 (Figure 9c) tumor cells at the same time of incubation. In human A375P cells, the percentage measurement of $C16^+$ -associated fluorescence revealed that, following 2 hours of contactless co-culture with $C16^+$ hEo5 or $C16^+$ hEo33, ~ 50% and ~ 85% of incorporation of the respective $C16^+$ hExo5 and $C16^+$ hExo33 were observed. By 18 h incubation, A375P cells had incorporated ~ 100% $C16^+$ hExo5 and $C16^+$ hExo33 (Figure 9d). These results indicate that mouse and human eosinophil-derived exosomes are efficiently transferred into target tumor cells and that in some tumor cells Exo33 are incorporated more rapidly with respect to Exo5.

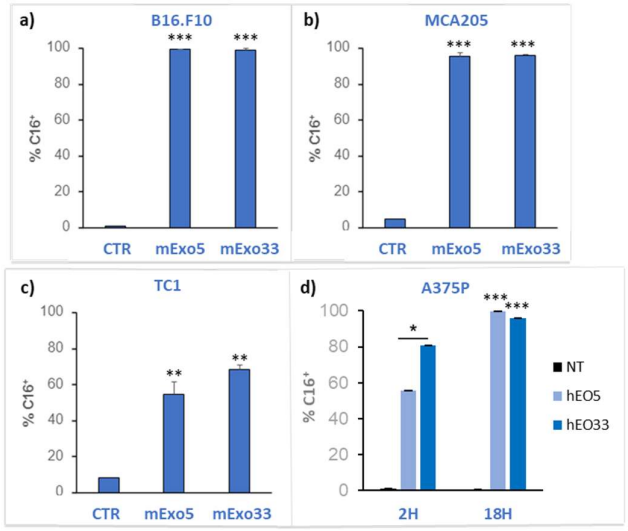

Figure 9. Flow cytometry analysis of fluorescent Exo uptake by tumor cells. Tumor cells were cultured alone or with Eo5 or Eo33 in 0.4 μm-pore sized transwell plates to avoid direct cell-cell contact, $C16^+$ mExo5 and $C16^+$ mExo33 internalization was evaluated within (a) B16.F10, (b) MCA205 and (c) TC1 following 2 hours incubation, while $C16^+$ hExo5 and $C16^+$ hExo33 internalization within (d) A375P was evaluated after 2 hours and 24 hours incubation. Mean values ±SD from triplicates and one representative experiment out of two are shown. **P<0.001, ***P<0.0001. One Way Anova analysis of variance with Tukey's Multiple Comparison Test.

4.5 *Exosomes from IL-33 activated eosinophils exert antiproliferative activities against tumor cells through cell cycle arrest*

Exo constitute a vesicle-mediated pathway employed by their producing cells to mediate, in an indirect manner, their activities. It is widely documented that once internalized, Exo are able to induce radical variations in gene expression of target cells, through the release of their molecular cargo, causing downstream signaling cascades (Deatherage et al., 2012; Thomou et al., 2017; Valadi et al., 2007). To determine whether eosinophil-derived Exo may affect tumor cell transcriptomic program and to investigate the possible role of Exo in mediating Eo33 anti-tumor activities, we exposed tumor cells to Exo5 or Exo33 and analyzed cell cycle inhibitor gene expression. Our qPCR results revealed that mouse B16.F10 melanoma cells up-regulated the expression of *Cdkn1b* when exposed to mExo33, but not to mExo5, and of *Cdkn2b* (that encodes for CDK inhibitor 2b), when cultured with mExo33 or with the whole Eo33 secretome (Sup mEo33) (Figure 10a).

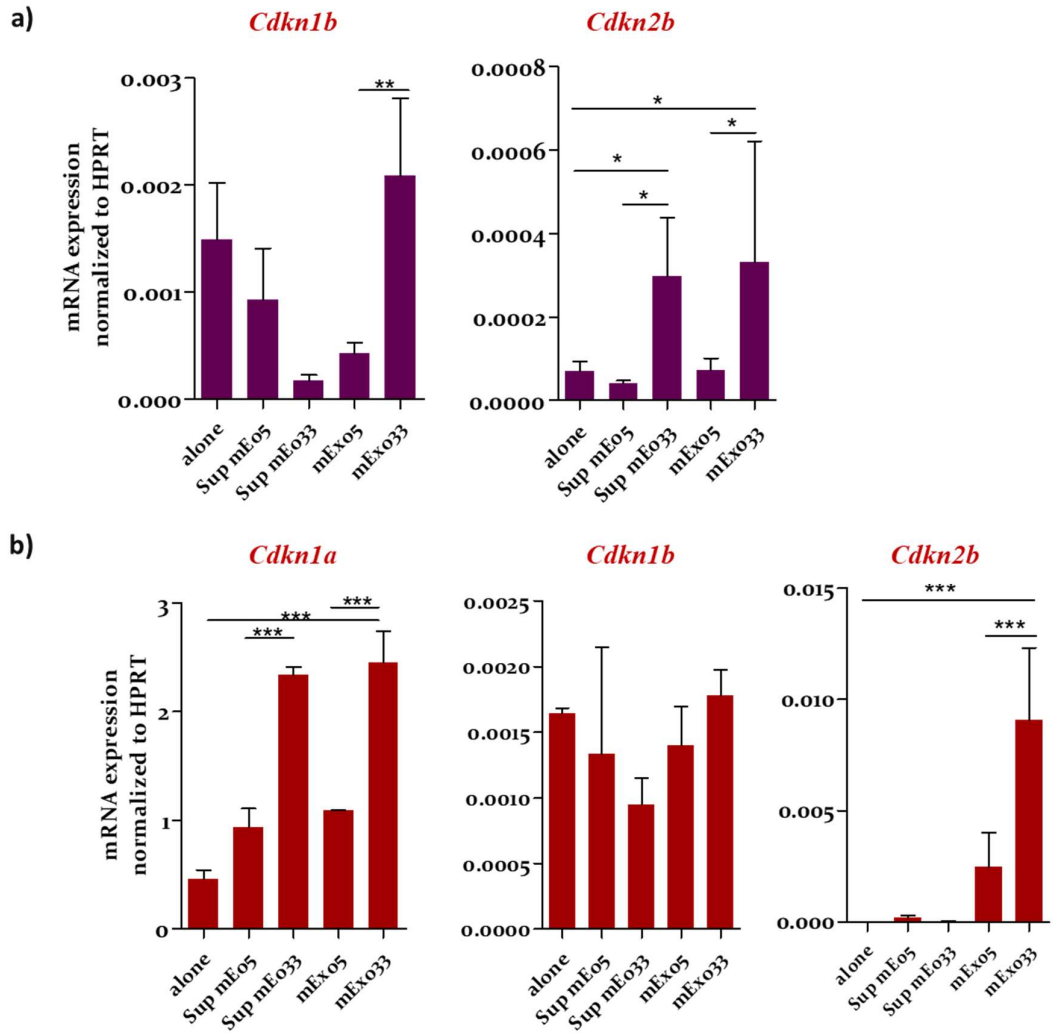

Figure 10. Gene expression analysis of the main cell cycle inhibitors (*Cdkn1a, Cdkn1b, Cdkn2b*) in (a) B16.F10 and (b) TC1 tumor cells cultured alone, with the whole secretome Sup mEo5 or Sup mEo33, with mExo5 or mExo33. Mean values ±SD from triplicates and one representative experiment out of three are shown. *P<0,05, **P<0.001, ***P<0.0001. One Way Anova analysis of variance with Tukey's Multiple Comparison Test.

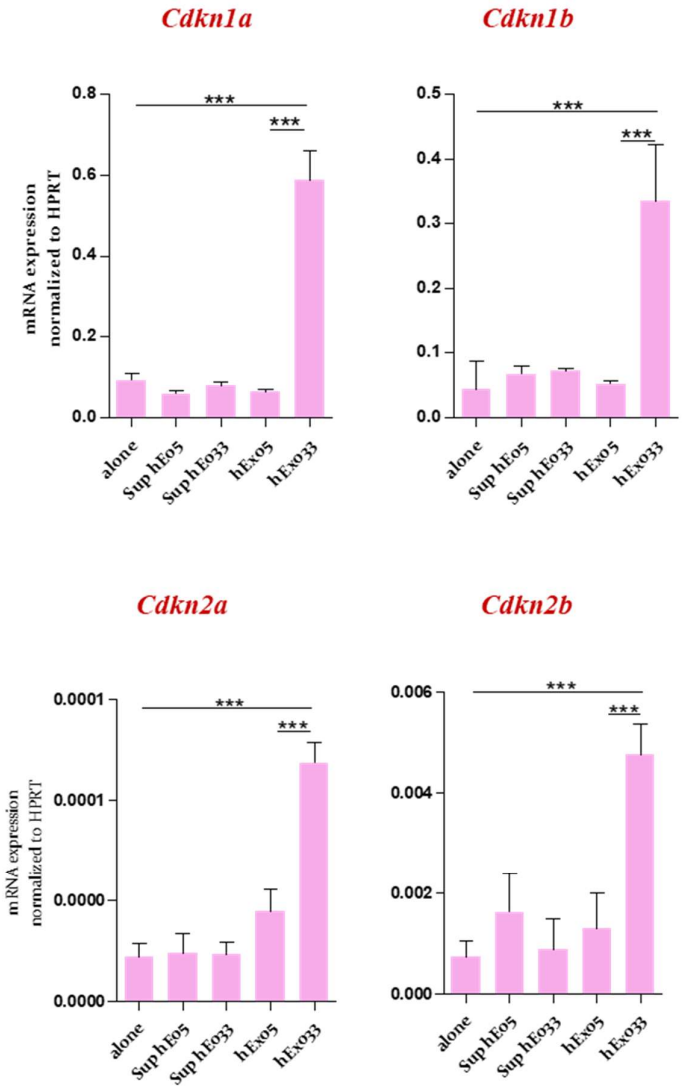

Figure 11. Gene expression analysis of the main cell cycle inhibitors (*Cdkn1a, Cdkn1b, Cdkn2a,Cdkn2b*) in A375P tumor cells cultured alone, with the whole secretome Sup hEo5 or Sup hEo33, with hExo5 or hExo33. ***P<0.0001. One Way Anova analysis of variance with Tukey's Multiple Comparison Test. Mean values ±SD from triplicates and one representative experiment out of two are shown.

Mouse TC1 lung adenocarcinoma cells up-regulated the expression of *Cdkn1a*, when exposed to either mExo33 or Sup mEo33, and of *Cdkn2b,* when exposed to mExo33. *Cdkn1b* expression does not appear to be modulated (Figure 10b). Human melanoma A375P cells treated with hExo33, but not with hExo5, significantly up-regulated the expression *Cdkn1a*, *Cdkn1b*, *Cdkn2a* (that encodes for CDK inhibitor 2a) and *Cdkn2b* genes (Figure 11). These results demonstrate that exposure to Eo33-derived exosomes modulates cell cycle inhibitor genes in a similar manner as observed with tumor cells

co-cultured with Eo33 and suggest a possible Exo involvement in cell cycle arrest which could eventually be translated into an inhibition of tumor cell proliferation.

Since these molecules are responsible for preventing the entry into the S phase of the cell cycle, it might be possible that Exo33 could block tumor cells in G0 phase. To address this hypothesis, we carried out cell cycle analysis by PI staining of tumor cells cultured alone or exposed to Exo5 or to Exo33. Flow cytometry analysis revealed that B16.F10 melanoma cells showed an increase of cell percentage at G0/G1 phase and a corresponding decrease in G2/M and S phases at 24 h, when cells were exposed to mExo33 but not in the other two control conditions (Figure 12a). Moreover, a significant increase in the percentage of tumor cells in G0 phase that significantly correlates with a lower percentage of cells in G2/M phase was observed at 24 h in TC1 adenocarcinoma cells exposed to mExo33 with respect to cells cultured alone or with mExo5 (Figure 12b). Similarly, in the human setting the percentage of A375P in G0 phase significantly increased while the percentages of cells in G2/M and S phases decreased after both 24 h and 48 h exposure to hExo33, with respect to the control conditions (Figure 12c).

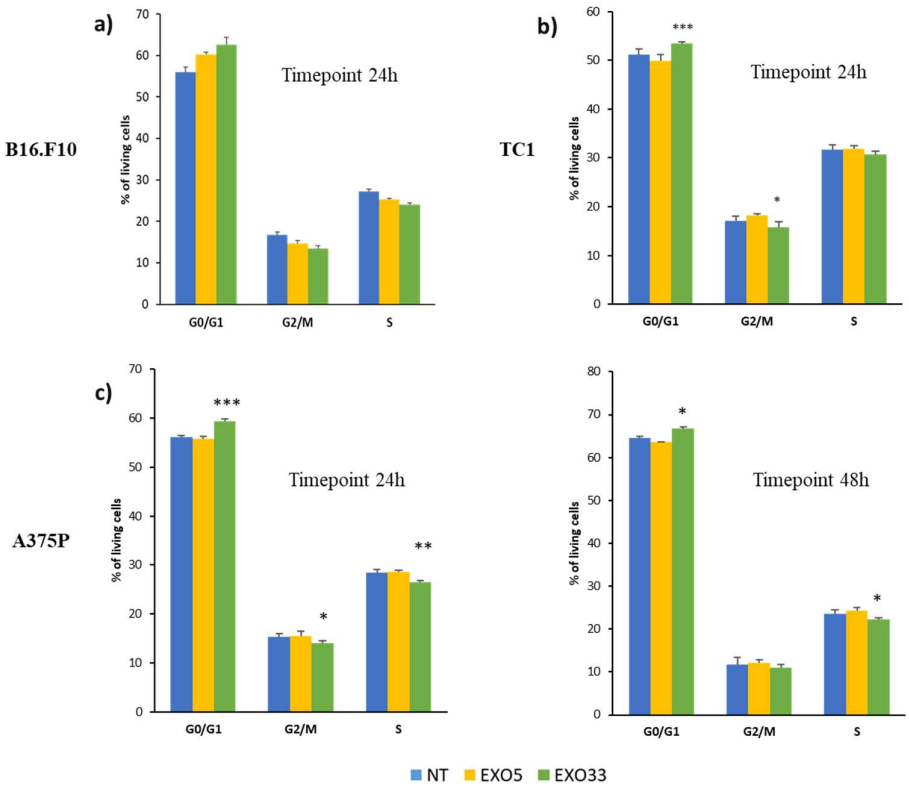

Figure 12. Cell cycle analysis by flow cytometry. Mouse and human tumor cells cultured alone (NT) or in the presence of Exo5 or Exo33 (mouse or human, respectively) were subjected to PI staining for cell cycle analysis. (a) B16.F10, 24 h; (b) TC1, 24h; (c) A375P, 24 h and 48 h. One representative experiment out of three and mean values ±SD from triplicates are shown. *P<0,05, **P<0.001, ***P<0.0001.

To evaluate whether an actual reduction of the proliferation rate of tumor cells occurred after exposure to Exo33, we performed an MTS assay. We observed that B16.F10 melanoma cells exhibited ~ 50% reduction of cell proliferation after 96 h exposure to mExo33 while MCA205 and TC1 cells displayed, ~ respectively, 15% and ~40% reduction in cell proliferation after 120 h exposure to mExo33 (Figure 13).

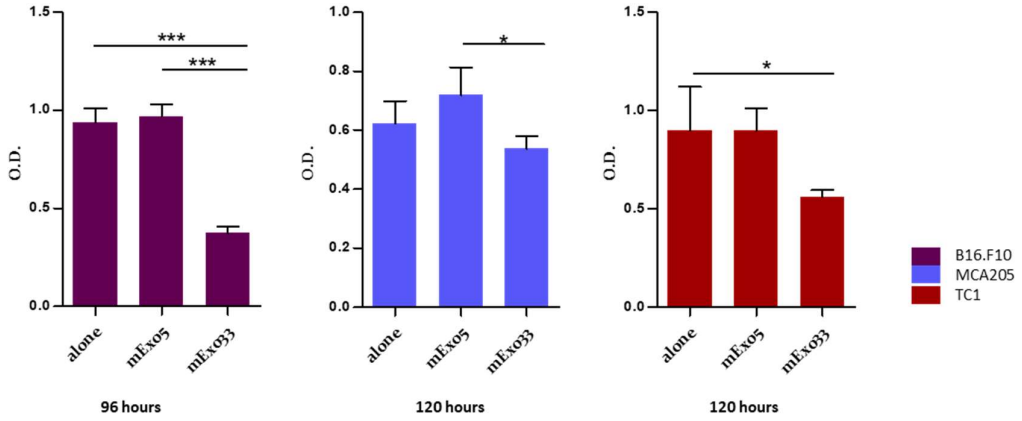

Figure 13. Analysis of tumor cell proliferation. MTS assay on mouse tumor cells (B16.F10: violet; MCA205: blue; TC1: red) cultured alone, with mExo5 or mExo33 at the indicated times. *P<0.05, ***P<0.0001. One representative experiment out of two and mean values ±SD from triplicates are shown.

Of interest, we observed that Exo secretion by mEo33 does not seem to affect the percentage of apoptotic melanoma cells (Figure 14a), since the inhibition of Exo secretion by eosinophil treatment with the pharmacological inhibitor GW4869 increased (rather than reduced) the percentage of apoptotic (Annexin V^+) melanoma cells (Figure 14b). Taken together, MTS and Annexin V assays revealed that Exo33 exert an anti-proliferative but not cytotoxic activity against tumor cells.

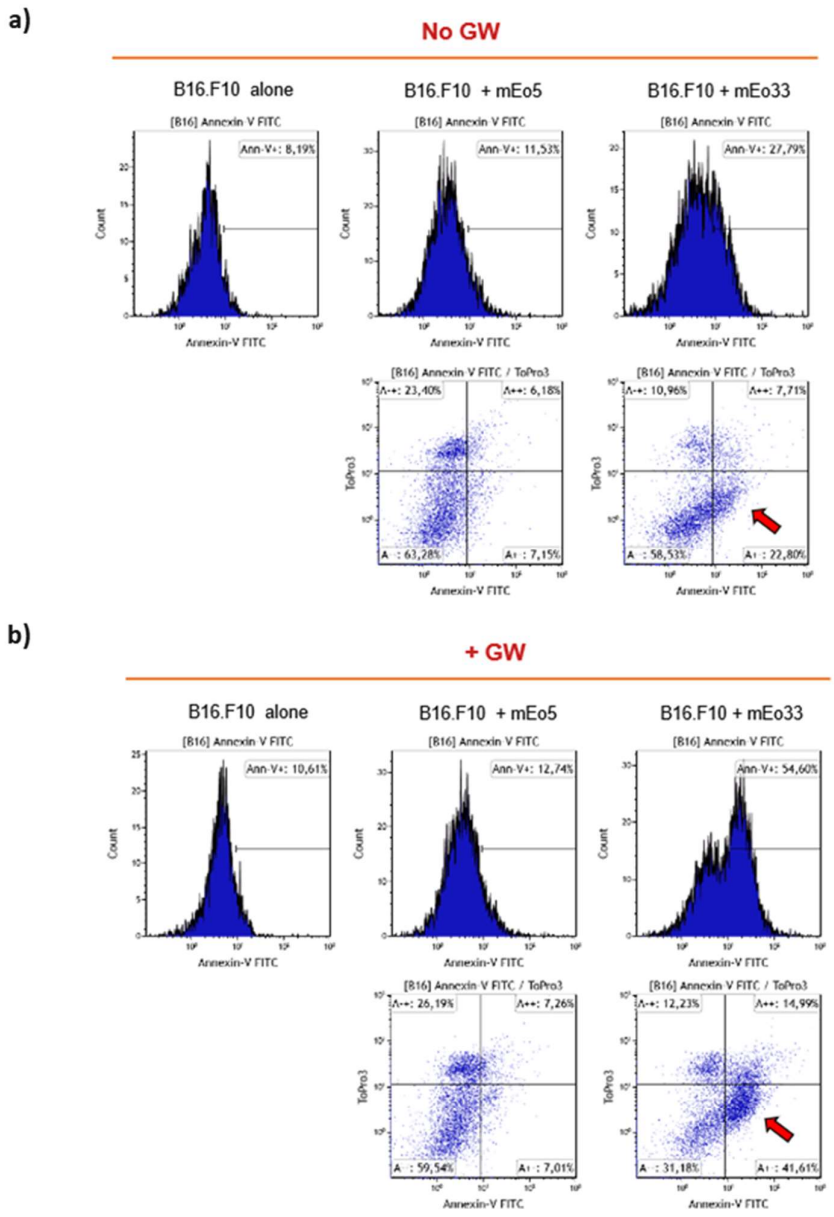

Figure 14. Flow cytometry analysis of tumor cell apoptosis. B16.F10 cells were cultured for 5 hours alone or with eosinophils (mEo5 or mEo33) either untreated (a) or previously treated with the inhibitor of exosome secretion GW 4869 (b). Apoptosis was detected by Annexin V/PI staining. One representative experiment out of two is shown.

4.6 *IL-33 activated eosinophil -derived exosomes inhibit the tumor spheroid formation*

Tridimensional (3D) cultures of tumor cells may reflect certain behaviors occurring during tumor progression and are currently employed for the study of drug sensitivity and stimuli responses. We carried out a 3D tumor spheroid formation assay to study the impact of Eo-derived Exo on the ability of tumor cells to interact with each other to form 3D spheroids. After four days of culture, B16.F10, TC1 and A375P tumor cells exhibited a strong capacity for cellular aggregation through the formation of a single tumor spheroid characterized by definite outline (Figure 15). Addition of Exo33 or Sup Eo33 markedly inhibited the single tumor spheroid formation, determined by loss of tumor cell aggregation capability, causing the formation of smaller cell aggregates (Figure 15). On the contrary, the exposure to Sup Eo5 or Exo5 did not alter the formation and 3D architecture of the tumor spheroids (Figure 15).

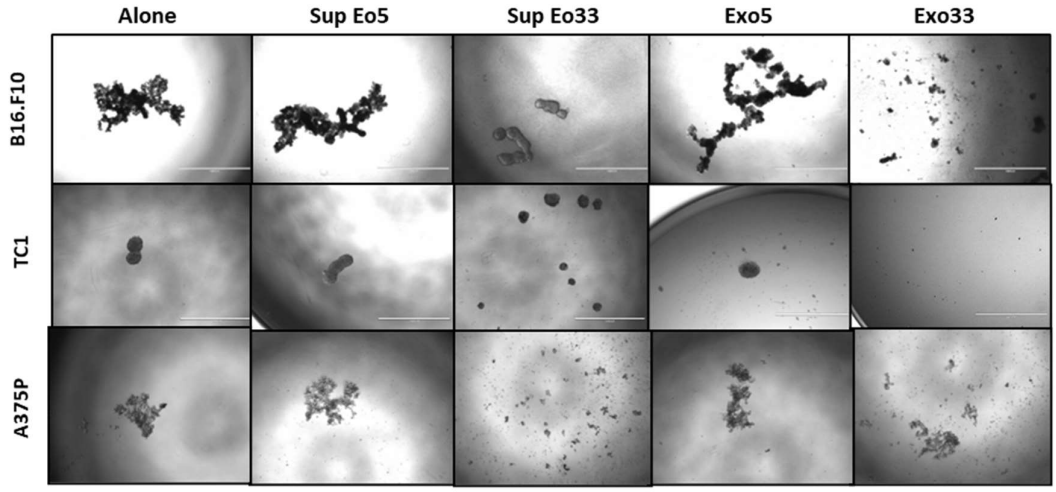

Figure 15. Effects of eosinophil-derived exosomes or whole secretome on the formation of tumor spheroids. The indicated mouse and human tumor cell lines were cultured in ultra-low attachment plates in medium alone or containing purified Eo5- or Eo33-Exo and to Eo5- or Eo33-supernatants. The formation of tumor spheroid was monitored over time by microscopy. Alone: tumor cells in fresh medium, Sup Eo5: tumor cells in 50% Eo-5 culture supernatant, Sup Eo33: tumor cells cultured in 50% Eo33 culture supernatant, Exo5: tumor cells in fresh medium with the addition of Eo5 –derived exosomes, Exo33: tumor cells in fresh medium with the addition of Eo33 –derived exosomes. Scalebar 1000 mm. Observation at day 4 by Evos microscope. One representative experiment out of three is shown.

In order to understand the possible mechanisms underlying the observed effect of Exo33 on tumor spheroid formation, gene expression analysis of the main molecules that

orchestrate cell adhesion pathways were performed. Integrins typically mediate epithelial cell adhesion to the basement membrane, but might contribute to migration, proliferation and survival of tumor cells (Desgrosellier et al. 2010). Gene expression analysis showed that A375P cells exhibited higher expression levels of *Itga2* ed *Itgb1* (genes coding for Integrin α2 and Integrin β1) after contact with hExo33 (Figure 16). TC1 cells up-regulated *Itga5* (gene coding for Integrin α5) and *Itgb1* following mExo33 treatment, with respect to tumor cells cultured alone or with Exo5 while B16.F10 cells showed increased levels in the expression of *Itga5* (Figure 16).

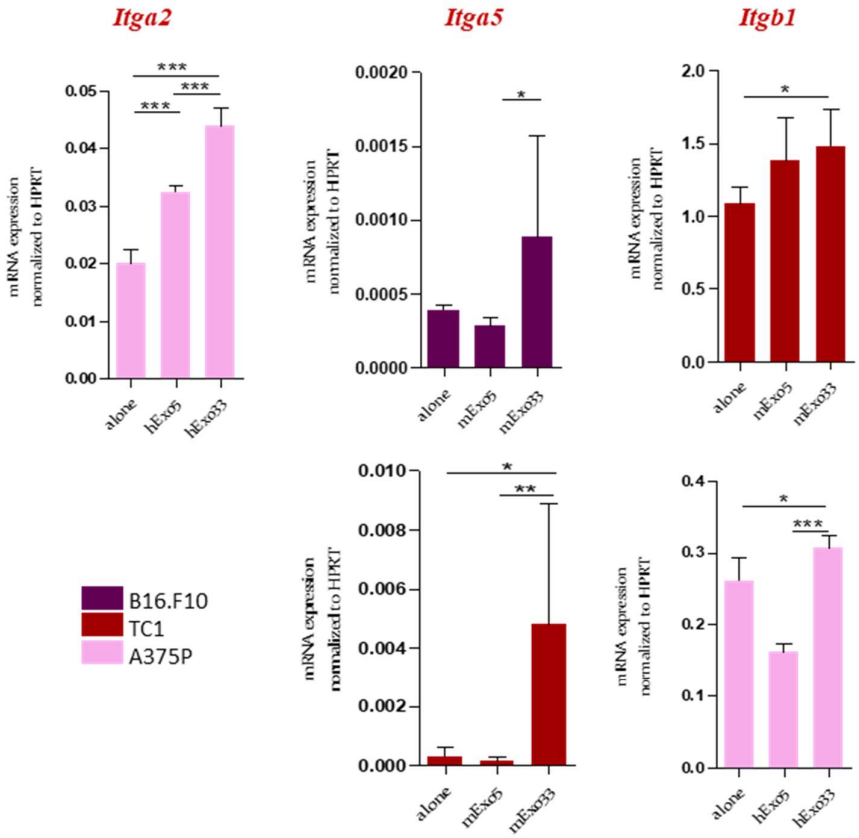

Figure 16. Gene expression analysis of the main integrins that orchestrate cell adhesion pathways (*Itga2, Itga5, Itgb1*) in mouse (B16.F10: violet, TC1: red) and human (A375P: pink) tumor cells cultured with mouse or human Exo5, Exo33 or left alone. Mean values ±SD from triplicates are shown. ***P<0.0001, **P<0.001, *P<0.05. One Way Anova analysis of variance with Tukey's Multiple Comparison Test.

4.7 *IL-33 activated eosinophil -derived exosomes modulate the expression of genes involved in epithelial to mesenchymal transition resulting in reduced tumor cell migratory ability*

In view of the above reported results on modulation of genes involved in EMT by Eo33, we investigated the role of exosomes in mediating these effects. Upon overnight exposure to mExo33, mouse B16.F10, MCA205 and TC1 tumor cells showed a significantly lower expression of *Cdh2* and, simultaneously, consistently higher expression of *Cdh1* (Figure 17). Similarly, up-regulation of *Cdh1* and down-regulation of *Cdh2* could be observed in A375P human melanoma cells following exposure to hExo33 but not to hExo5 or in untreated cells (Figure 17). These data suggest that activation of mouse or human eosinophils with IL-33 modulate the expression of EMT markers towards an inhibition of tumor progression and/or malignant phenotype through the release of exosomes.

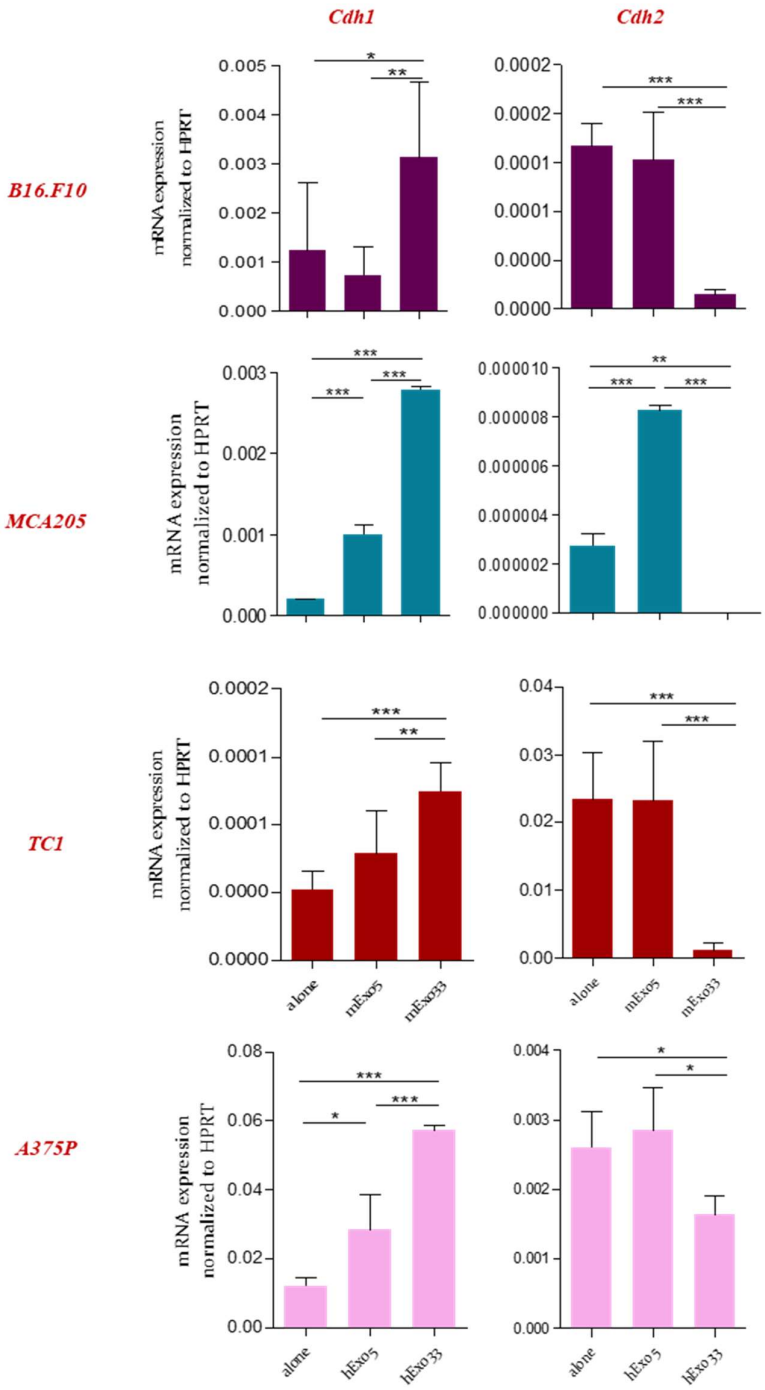

Figure 17. Gene expression analysis of the main markers that orchestrate epithelial to mesenchymal transition (*Cdh1* and *Cdh2*) in mouse (B16.F10: violet, MCA205: green, TC1: red) and human (A375P: pink) tumor cells exposed to Exo5, Exo33 or left alone. Mean values ±SD from triplicates and one representative experiment out of three are shown. ***P<0.0001, **P<0.001, *P<0.05. One Way Anova analysis of variance with Tukey's Multiple Comparison Test.

The Exo33-triggered inhibition of migratory potential of tumor cells was functionally confirmed in a wound healing scratch assay, in which B16.F10 melanoma cells were tested for their capacity to recolonize a scratched region by cell migration/motility following exposure to mExo5 or mExo33. Time lapse images at 24 h and 48 h show that while tumor cells cultured alone or with Exo5 almost completely invaded and closed the scratched area, tumor cells exposed to mEo33 exhibited a greater scratched cell-free area (Figure 18). These findings support the hypothesis that Exo33 could play a role in reshaping tumor cell phenotype toward a less metastatic and invasive features, by inhibiting the epithelial to mesenchymal transition process.

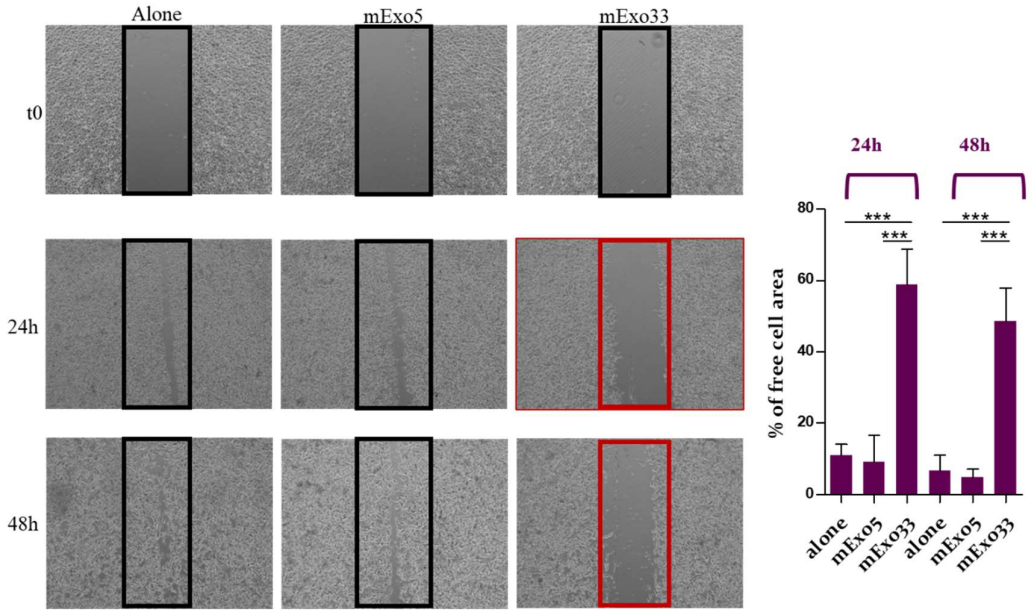

Figure 18. Evaluation of metastatic and migratory potential, through wound healing scratch assay. Mouse B16.F10 melanoma cells were cultured alone or in the presence of mExo5 or mExo33 for 24 h and then scratched. Percentage of wound healing by tumor cells was kinetically monitored over time by Evos microscopy. Scalebar 1000 mm. Observation at time 0h, 24h, 48h. Micrographs were analysed by ImageJ Software. Mean values ±SD from triplicates and one representative experiment out of three are shown. ***P<0.0001. One Way Anova analysis of variance with Tukey's Multiple Comparison Test.

4.8 *Comparative analysis of Exo5 versus Exo33 molecular content by RNA-Seq*

The molecular cargo carried by Exo that reflects the nature of donor cell and induces downstream signaling cascades when transferred into recipient cells (Deatherage et al., 2012; Doyle et al., 2019). To discover the molecular content enclosed within eosinophil-derived Exo and to study their possible involvement in the observed effects on cancer cells, we carried out RNA-Seq on mExo5 and mExo33 and on their respective producing cells (mEo5 and mEo33). RNA-Seq identified 149223 transcripts in our samples, which included 101830 mRNAs. We cross-filtered mRNA transcripts mainly expressed in exosomes (either mExo5 or mExo33), which simultaneously displayed a similar behavior in their producing cell (mEo5 or mEo33, respectively). Through this process, we identified a cluster of 16 mExo5 transcripts (*Paics, Tead2, Rasal3, Smc2, Rc3h2, Xylt2, Dpf2, Atp8a2, Brca1, Nek6, Pnpla7, Mprip, Banp, Pnn, Dcaf13* and *Cacul1*), whose cell behavior is similar in mEo5 (Table I; Table II; Figure 19A). Concomitantly, a cluster of 22 mExo33 transcripts (*Efemp1, Dct, Tmprss15, Slc18a2, Nkd1, Fam124a, Slc24a2, Slc25a43, Cldn14, Pcsk6, Kcns3, Sh3rf2, Lrp2, Hirip3, Zmat4, Tecpr1, Slc22a22, Myo6, Ro60, Ppfibp2, Adtrp* and *Hecw1*) whose cell behavior is similar in mEo33 (Table I; Table II; Figure 19A). Hierarchical clustering analysis on heatmap data (Figure 19B) clearly suggest a close similarity between the two experimental replicates (R1, R2) within each condition (mExo33, mExo5). Moreover, two distinct gene clusters have been identified for the two mExo5 and mExo33 experimental conditions. Indeed, both hierarchically clustered mExo33 and mExo5 transcript profiles display a cluster of genes poorly expressed or not expressed, which can be intended as a cluster of transcripts exclusives for either mExo33 or mExo5 (bottom clusters in Figure 19B).

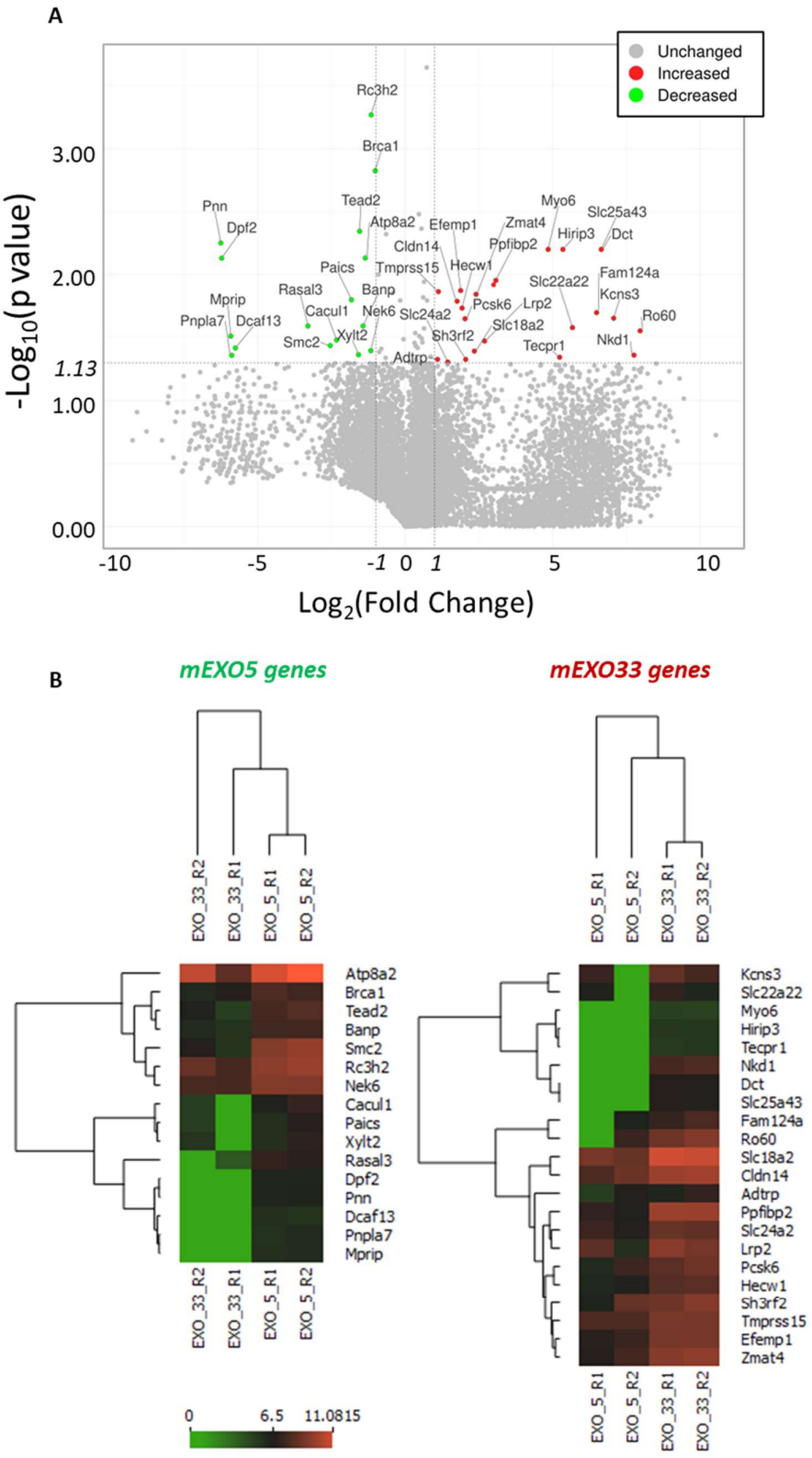

Figure 19. Transcriptomic analysis by bulk RNA sequencing. Differential expression of mExo5 genes and mExo33 genes represented: A) in Volcano Plot, in which 16 green plots are referred to the 16 mExo5 genes while 22 red plots are referred to the 22 mExo33 genes, and; B) in heatmaps with a hierarchical clusterization of genes (rows) and experimental conditions (rows) by similarity. Statistical analysis with Ttest was performed. P-value <0.05.

Data from GO analysis indicate that mExo5 transcripts are significantly associated to a set of pathways leading to increase of cell proliferation and pro-tumoral activity (Figure 20). Indeed, several pathways extrapolated by this LAGO analysis are generally associated to cell cycle activation (i.e., “cell growth”, “mitotic cell cycle” and “positive regulation of cell cycle”, Figure 20A). Moreover, other pathways such as “embryonic organ development”, “p53 binding” and “blood vessel morphogenesis” represent key processes supporting cancer generation and development (Ausprunk et al., 1977). Conversely, the mExo33 mRNA set is clearly involved in a plethora of processes favoring the inhibition or delay of cell proliferation and a general decrease of cell activity. For example, mExo33 transcripts appear to be involved in processes closely related to the formation and secretion of extracellular vesicles (“receptor-mediated endocytosis”, “cargo receptor activity”, “transmembrane transporter activity” and “cell-cell signaling processes”) (Figure 20B; Gurung et al., 2021; Perez-Hernandez et al., 2013).To further explore the representative role of anti-proliferative process dominance in mExo33 genes compared to mExo5 ones, the two mRNA sets were subjected to G-profiler analysis. As expected, findings from G-Profiler support the LAGO pathway profiling results. Indeed, a larger number of significantly active pathways has been found for mExo5 genes (n=27) compared to the concomitant active processes in mExo5 genes (n=10) (G-profiler; Figure 20).

In summary, the profiles extrapolated by mExo33 and mExo5 mRNA sets are in line with our functional experiments showing that Exo33, but not Exo5, exert anti-proliferative activity and prevent malignant progression when incorporated into tumor cells.

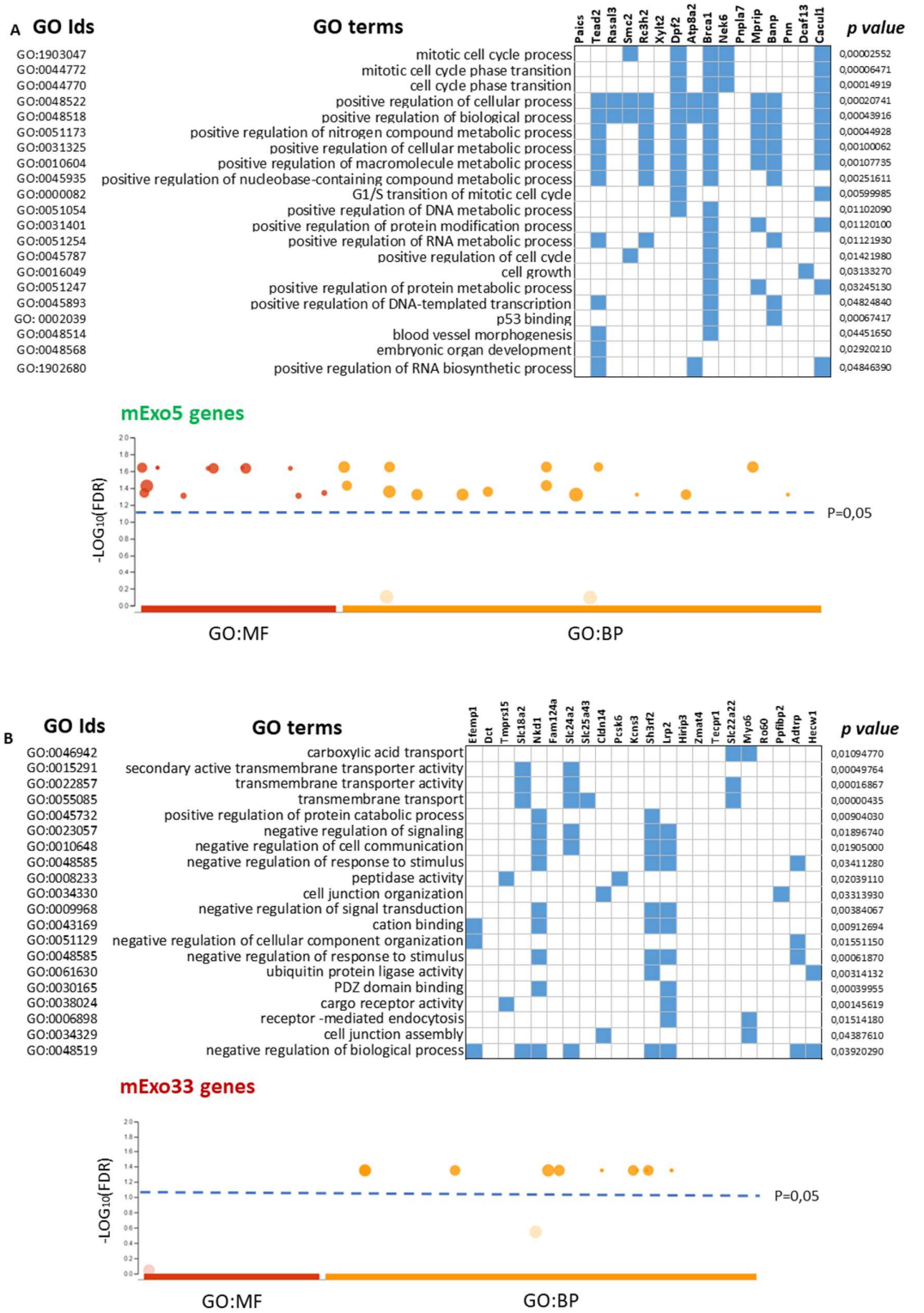

Figure 20. Table of LAGO GO analisys and G:profiler graphical representation of the biological processes in which (A) mExo5 genes are involved by supporting tumor cell activity and (B) mExo33 genes are involved by inactivating tumor cell activity. GO Ids, GO terms and gene names are reported. MF, molecular function; BP, biological process. Statistical analysis with Ttest was performed. P-value <0.05. Dashed line, p-value cut off.

5. DISCUSSION

Despite the controversial role of IL-33 in cancer immunity, it is extensively demonstrated that this epithelial-derived alarmin may provide anticancer responses in a number of tumors due to its ability to stimulate a wide set of immune cells, such as $CD8^+$ T cells, NK, DCs and eosinophils that infiltrate the TME (Mattei et al., 2020). Eosinophils have emerged as important components of the TME exerting several functions against cancer, ranging from the secretion of soluble mediators (i.e., chemokines) that facilitate the recruitment of $CD8^+$ T cells at the tumor site to cytotoxic degranulation (Mattei et al., 2020; Grisaru-Tal et al., 2021). On the other hand, eosinophils can secrete several pro-angiogenic factors, such as VEGF-A, fibroblast growth factor (FGF-2), CXCL8/IL-8, which may favor tumor progression (Varricchi et al., 2018). In this scenario, exosomes as conveyors of molecular messages may intervene providing communication between tumor, nonimmune and immune cells and mediating the activities of their producing cell (Deatherage et al., 2012; Doyle et al., 2019). Exosomes are involved in various biological processes and play a central role in cancer (Osaki et al., 2019) by conveying pro- or anti-tumoral messages, depending on the type and status of the producing cell, which affect the molecular cargo delivered by exosomes (Filipazzi et al., 2012; Zech et al., 2012; Boussadia et al., 2021; Yang et al., 2020).

In our previous work, we demonstrated that IL-33-activated eosinophils exhibit strong tumoricidal activity against tumor cells in mouse models *in vitro* and *in vivo* (Lucarini et al., 2017; Andreone et al., 2019). Direct contact of IL-33-activated, but not IL-5-activated, eosinophils resulted in synapse polarized degranulation and tumor apoptosis, albeit not in all cancer cells. This latter evidence has led to the hypothesis that further mechanisms underlying antitumoral functions of IL-33 activated eosinophils could arise. In the present study, we show that in mouse and in human tumor cells, the direct contact with IL-33 activated eosinophils, respectively mouse and human, was also responsible for changes in tumor cell expression of genes involved in tumor progression.

First, tumor cells cultured with Eo33 exhibited increased levels in the expression of cyclin dependent kinase inhibitors (CDKI), such as *CDKN1A, CDKN2A; CDKN1B, CDKN2B*, suggesting a possible propensity to cell cycle blockade (Leal-Esteban et Fajas, 2020). Aberrancies in cell cycle regulatory proteins have been defined in all types

of human cancers and result in uncontrolled proliferation and tumor progression. A prominent role in blocking cancer development is achieved by acting on cell cycle blockade where CDKI arrest cell cycle progression in G0/G1 phase and therefore tumor proliferation (Engeland, 2022; Liu et al., 2022).

Furthermore, analysis of the main molecules (E-Cadherin and N-Cadherin) that regulate the epithelial to mesenchymal transition (Loh et al., 2019) denoted a reversion of this process in mouse and human tumor cells co-cultured with Eo33, indicating that tumor cells might be less prone to tumor dissemination. In fact, co-culture with Eo33 induced significantly higher expression of E-Cadherin both at transcriptional and surface protein expression, with respect to Eo5. Concomitantly, Eo33 produced in target tumor cells significantly more marked down-modulation of N-Cadherin compared to Eo5. The observation that the upregulation of E-Cadherin expression on mouse tumor cell surface occurred also in absence of direct contact with Eo33, led us to evaluate the possible involvement of an exosome-mediated pathway in the anticancer functions of IL-33 activated eosinophils.

It has been described that eosinophils secrete functional exosomes following activation with IFN-γ and that the release of exosomes is higher in eosinophils from asthmatics compared to healthy individuals (Mazzeo et al., 2015). Moreover, eosinophil-derived exosomes participate in asthmatic airway remodeling by affecting inflammation-related gene expression in target cells (Cañas et al., 2018). Here, we observed that stimulation with IL-33 also increased the secretion of exosomes by both mouse and human eosinophils, as demonstrated by flow cytometry-based enumeration of metabolically labeled $C16^{+}$ Exo (Coscia et al., 2016). This finding, together with previous reports (Rodrigo-Munoz et al., 2021), suggest that activation stimuli promote exosome secretion by eosinophils resulting in enhanced potential to shape target cells or tissues. In fact, the quantity of secreted Exo depends on whether cells are experiencing different stressors or stimuli (Kalluri et al., 2016).

Once incorporated into recipient cells, Exo act by altering cellular physiology (Joshi et al., 2020; Tian et al., 2013) through the activation of downstream signaling cascades that in turn result in switching on and off a number of genes (Deatherage et al., 2012; Horibe et al., 2018; Santos et al., 2018; Gurung et al., 2021). Depending on the specific cases, Exo-triggered transcriptional regulation can be disease promoting or suppressing (Kalluri et al., 2016). We found that mouse and human IL-33 activated eosinophil-derived exosomes carry out antitumoral activities by influencing the transcriptional

machinery of target tumor cells. Tumor progression represents a dense network of multiphasic proceedings that may result in the constitutive activation of genes involved in uncontrolled cell proliferation and redundant cell cycle events (Arneth, 2019; Evan et Vousden, 2001). We demonstrate that Eo33 drive the expression of CDKI genes in mouse and human tumor cells through the release of exosomes. This transcriptional reprogramming corresponded to cell cycle block in G0/G1 phase and an effective decrease in the proliferative rate of cancer cells, as suggested by flow cytometry experiments and MTS assay. Of note, the anti-proliferative effects of Exo33 did not seem to involve tumor apoptosis, as suggested by Annexin V^+ staining of tumor cells cultured with GW exosome inhibitor-treated Eo33.

Thus, Exo33 may control tumor progression by suppressing tumor cell proliferation intervening in the transcriptional activation of genes that conduct to cell cycle blockade but are not involved in the tumoricidal activity of IL-33 activated eosinophils, which is degranulation dependent. Furthermore, the most rapid incorporation of $C16^+$ Exo33, with respect to C16+ Exo5, within tumor cells, both in mouse and human settings, may contribute to the observed anti-tumor effects induced by Exo33.

Tumor 3D cultures provided some details of the impact of Eo33 -derived Exo on the ability of tumor cells to interact with each other to form single 3D spheroids. In mouse and human setting, the observation that Exo33 or Sup Eo33 altered the formation and 3D architecture of the tumor spheroid by acting on tumor cell aggregation capability has inspired us to perform gene analysis of the expression of the main molecules that regulate cell adhesion pathways. We found increased expression of membrane integrins in mouse and human tumor cells exposed to Exo33 or to Eo33-derived secretome.

Besides playing an important role in mediating epithelial cell adhesion to the basement membrane, integrins are involved also in migration, proliferation and survival pathways of tumor cells (Desgrosellier et al. 2010). Some studies indicate the controversial role and the contradictory data either within the same cancer type or in relation to different cancers for the same integrin molecules (Hamidi et al., 2018). Further reports showed that the pro-tumorigenic integrin αvβ3 could inhibit tumor progression in some mouse models of glioblastoma and melanoma (Danen et al., 1996), while other integrins inhibit tumor cell motility. It was reported that integrin β1 (Itgb1) deletion correlates with increased tumor cell dissemination in a mouse model of spontaneous pancreatic islet cancer and others such as a5β1 inhibit oncogene-induced transformation (Desgrosellier et al. 2010). Therefore, the modulation of integrin expression did not provide exhaustive

details about acquired variations in their propensity in metastatic potential following exposure to Exo33. Nevertheless, our observations on EMT markers modulation as well as scratch assay experiments indicate that Exo33 may shape tumor cells towards a less aggressive phenotype. In fact, Exo from either mouse and human Eo33 significantly increased *Cdh1* expression while down-modulated *Cdh2* in target tumor cells, with respect to Exo5 or the control condition. This transcriptional trait correlated with the lower invasive propensity of cancer cells, following Exo33 incorporation, which confirmed a plausible inhibition of EMT, a key process driving metastatic spread (Zhao et al., 2016; Alt-Holland et al., 2008; Loh et al., 2019).

Our RNA-Seq analysis are in line with the functional experiments showing that tumor cells exposed to mExo33, but not to mExo5, modulated the expression of genes involved in tumor suppression, resulting in reduced tumor cell migratory ability and cell cycle arrest. By bioinformatic workflow, two clusters of 16 and 22 mRNAs, mostly expressed in mExo5 or mExo33, respectively, were successfully identified from a total of 149223 sequenced transcripts. Notably, LAGO and G-profiler essential GO terms discriminated a set of biological processes leading to pro-tumoral activities in which mExo5 transcripts seem to be involved as opposed to biological processes leading to a possible general decrease of tumor cell activities in which mExo33 transcripts appear to be involved. Specifically, mRNAs preferentially expressed in mExo5 may directly act on cell cycle enhancement through a positive regulation, while other of these have been reported to be associated with the blood vessel morphogenesis and p53 binding processes. In particular, the association of mExo5 *Tead2* gene with “embryonic organ development” process suggested that this mRNAs may also play a role in EMT transition. It is widely reported that EMT is a crucial event intervening in embryonic development and enables polarized epithelial cells to transition toward a mesenchymal phenotype with increased cellular motility. These two processes have in common a wide array of orchestrating molecules and, together with tissue repair, may intervene in cancer progression due to their known properties to confer malignant features to carcinoma cells, such as invasive behavior, cancer stem cell activity and greater resistance to chemotherapy and immunotherapy (Lu and Kang., 2019).

Blood vessel morphogenesis, in which seems to be involved *Tead2*, is a crucial event that supports angiogenesis and metastatic spread (Wenes et al., 2016) and has been widely accepted as a basic mechanism of angiogenesis in wound healing and in tumors (Ausprunk et al., 1977). On the other hand, *Brca1* and *Banp* mExo5 transcripts interact

with p53 oncosuppressor gene. Mutations are widely reported in cancer and may turn off p53 activity resulting in their loss of function. Particularly, *Banp* encodes a protein that binds to matrix attachment regions. The protein forms a complex with p53 and negatively regulates p53 transcription. When inhibited, the oncosuppressor p53 loses its ability to counteract the uncontrolled proliferation by blocking cell cycle events. Moreover, the cell is then unable to inhibit uncontrolled and noncanonical proliferation, to preserve cell stability and to preventing mutations. These events are known to lead to cancer initiation process (Liebl et al., 2021). The silencing of circ-*Banp* markedly inhibited proliferation, migration and invasion of lung cancer cells *in vitro* and impaired tumor propagation *in vivo*. *Banp* expression was associated with lower survival rate and circ-*Banp*-mediated miR-503/LARP1 signaling promoted lung cancer growth, migration and invasion, providing a novel insight on the mechanism underlying lung cancer progression (Han et al., 2018).

Conversely, mExo33 transcripts (*Tmprss15, Slc18a2, Slc24a2, Slc22a2 and Myo6)* appear to be involved in processes closely related to the formation and secretion of extracellular vesicles, such as "receptor-mediated endocytosis", "cargo receptor activity" and "transmembrane transporter activity" (Gurung et al., 2021; Perez-Hernandez et al., 2013). Of note, we previously described that in IL-33 activated eosinophils the enhancement of their exosome secretion might lead to increased exosome activity. Surprisingly, some of the transcripts preferentially expressed in mExo33 (*Cldn14, Myo6 and Ppfibp2*), and less expressed in mExo5, seem to be involved in processes deputed to cell junction organization and cell-cell junction assembly, such as tight junction, adherents junction and desmosomes, that link cells to each other in tissues, regulate tissue homeostasis in critical cell processes that include tissue barrier functions. Defects in cell-cell junctions give rise to a wide range of tissue abnormalities that disrupt homeostasis and are common in genetic abnormalities and cancers (Garcia et al., 2018; Figure 20B). This observation may lead with the suggested Exo33 activity in reshaping tumor cell phenotype toward a less metastatic and invasive features, by inhibiting the EMT process. Through GO analysis, we found that mExo33 transcripts (*Nkd1, Sh3rf2 and Lrp2*) were reported to be associated with "negative regulation of signaling" that may lead to a possible decrease of tumor cell activities, resulting in anti-cancer outcomes.

The intrinsic properties of Exo in regulating intracellular pathways have advanced their potential utility in the therapeutic control of many diseases and particularly in cancer.

The future of exosome -based therapy includes combinations of targeted exosomes with anticancer drugs and high-precision cancer diagnostic probes to construct multifunctional platforms for *in vivo* tracking, prognosis monitoring and cancer therapy (Liang et al., 2020). In conclusion, our study provides a possible mechanism by which IL-33 stimulates the anticancer activities of eosinophils through exosome-mediated reprogramming of tumor cells.

6. REFERENCES

Abels ER, Breakefield XO. Introduction to Extracellular Vesicles: Biogenesis, RNA Cargo Selection, Content, Release, and Uptake. Cell Mol Neurobiol. 2016 Apr;36(3):301-12. doi: 10.1007/s10571-016-0366-z. Epub 2016 Apr 6. PMID: 27053351; PMCID: PMC5546313.

Abusamra AJ, Zhong Z, Zheng X, Li M, Ichim TE, Chin JL, Min WP. Tumor exosomes expressing Fas ligand mediate CD8+ T-cell apoptosis. Blood Cells Mol Dis. 2005 Sep-Oct;35(2):169-73. doi: 10.1016/j.bcmd.2005.07.001. PMID: 16081306.

Afferni C, Buccione C, Andreone S, Galdiero MR, Varricchi G, Marone G, Mattei F, Schiavoni G. The Pleiotropic Immunomodulatory Functions of IL-33 and Its Implications in Tumor Immunity. Front Immunol. 2018 Nov 13;9:2601. doi: 10.3389/fimmu.2018.02601. PMID: 30483263; PMCID: PMC6242976.

Akimoto M, Takenaga K. Role of the IL-33/ST2L axis in colorectal cancer progression. Cell Immunol. 2019 Sep;343:103740. doi: 10.1016/j.cellimm.2017.12.014. Epub 2018 Jan 9. PMID: 29329638.

Alt-Holland A, Shamis Y, Riley KN, DesRochers TM, Fusenig NE, Herman IM, Garlick JA. E-cadherin suppression directs cytoskeletal rearrangement and intraepithelial tumor cell migration in 3D human skin equivalents. J Invest Dermatol. 2008 Oct;128(10):2498-507. doi: 10.1038/jid.2008.102. Epub 2008 Jun 5. PMID: 18528437; PMCID: PMC2827766.

Andreone S, Spadaro F, Buccione C, Mancini J, Tinari A, Sestili P, Gambardella AR, Lucarini V, Ziccheddu G, Parolini I, Zanetti C, D'Urso MT, De Ninno A, Businaro L, Afferni C, Mattei F, Schiavoni G. IL-33 Promotes CD11b/CD18-Mediated Adhesion of Eosinophils to Cancer Cells and Synapse-Polarized Degranulation Leading to Tumor Cell Killing. Cancers (Basel). 2019 Oct 26;11(11):1664. doi: 10.3390/cancers11111664. PMID: 31717819; PMCID: PMC6895824.

Arneth B. Tumor Microenvironment. Medicina (Kaunas). 2019 Dec 30;56(1):15. doi: 10.3390/medicina56010015. PMID: 31906017; PMCID: PMC7023392.

Arnold IC, Artola-Borán M, Tallón de Lara P, Kyburz A, Taube C, Ottemann K, van den Broek M, Yousefi S, Simon HU, Müller A. Eosinophils suppress Th1 responses and restrict bacterially induced gastrointestinal inflammation. J Exp Med. 2018 Aug 6;215(8):2055-2072. doi: 10.1084/jem.20172049. Epub 2018 Jul 3. PMID: 29970473; PMCID: PMC6080907.

Arnoult D, Soares F, Tattoli I, Girardin SE. Mitochondria in innate immunity. EMBO Rep. 2011 Sep 1;12(9):901-10. doi: 10.1038/embor.2011.157. PMID: 21799518; PMCID: PMC3166463.

Ausprunk DH, Folkman J. Migration and proliferation of endothelial cells in preformed and newly formed blood vessels during tumor angiogenesis. Microvasc Res. 1977 Jul;14(1):53-65. doi: 10.1016/0026-2862(77)90141-8. PMID: 895546.

Bang C, Batkai S, Dangwal S, Gupta SK, Foinquinos A, Holzmann A, Just A, Remke J, Zimmer K, Zeug A, Ponimaskin E, Schmiedl A, Yin X, Mayr M, Halder R, Fischer A, Engelhardt S, Wei Y, Schober A, Fiedler J, Thum T. Cardiac fibroblast-derived microRNA passenger strand-enriched exosomes mediate cardiomyocyte hypertrophy. J Clin Invest. 2014 May;124(5):2136-46. doi: 10.1172/JCI70577. Epub 2014 Apr 17. PMID: 24743145; PMCID: PMC4001534.

Bebelman MP, Bun P, Huveneers S, van Niel G, Pegtel DM, Verweij FJ. Real-time imaging of multivesicular body-plasma membrane fusion to quantify exosome release from single cells. Nat Protoc. 2020 Jan;15(1):102-121. doi: 10.1038/s41596-019-0245-4. Epub 2019 Dec 13. PMID: 31836866.

Berchem G, Noman MZ, Bosseler M, Paggetti J, Baconnais S, Le Cam E, Nanbakhsh A, Moussay E, Mami-Chouaib F, Janji B, Chouaib S. Hypoxic tumor-derived microvesicles negatively regulate NK cell function by a mechanism involving TGF-β and miR23a transfer. Oncoimmunology. 2015 Jun 24;5(4):e1062968. doi: 10.1080/2162402X.2015.1062968. PMID: 27141372; PMCID: PMC4839360.

Binenbaum Y, Fridman E, Yaari Z, Milman N, Schroeder A, Ben David G, Shlomi T, Gil Z. Transfer of miRNA in Macrophage-Derived Exosomes Induces Drug Resistance in Pancreatic Adenocarcinoma. Cancer Res. 2018 Sep 15;78(18):5287-5299. doi: 10.1158/0008-5472.CAN-18-0124. Epub 2018 Jul 24. PMID: 30042153.

Boraschi D, Italiani P, Weil S, Martin MU. The family of the interleukin-1 receptors. Immunol Rev. 2018 Jan;281(1):197-232. doi: 10.1111/imr.12606. PMID: 29248002.

Boussadia Z, Gambardella AR, Mattei F, Parolini I. Acidic and Hypoxic Microenvironment in Melanoma: Impact of Tumour Exosomes on Disease Progression. Cells. 2021 Nov 25;10(12):3311. doi: 10.3390/cells10123311. PMID: 34943819; PMCID: PMC8699343.

Boyle EI, Weng S, Gollub J, Jin H, Botstein D, Cherry JM, Sherlock G. GO::TermFinder--open source software for accessing Gene Ontology information and finding significantly enriched Gene Ontology terms associated with a list of genes. Bioinformatics. 2004 Dec 12;20(18):3710-5. doi: 10.1093/bioinformatics/bth456. Epub 2004 Aug 5. PMID: 15297299; PMCID: PMC3037731.

Bu N, Wu H, Sun B, Zhang G, Zhan S, Zhang R, Zhou L. Exosome-loaded dendritic cells elicit tumor-specific CD8+ cytotoxic T cells in patients with glioma. J Neurooncol. 2011 Sep;104(3):659-67. doi: 10.1007/s11060-011-0537-1. Epub 2011 Feb 19. PMID: 21336773.

Buder-Bakhaya K, Hassel JC. Biomarkers for Clinical Benefit of Immune Checkpoint Inhibitor Treatment-A Review From the Melanoma Perspective and Beyond. Front Immunol. 2018 Jun 28;9:1474. doi: 10.3389/fimmu.2018.01474. PMID: 30002656; PMCID: PMC6031714.

Bunggulawa EJ, Wang W, Yin T, Wang N, Durkan C, Wang Y, Wang G. Recent advancements in the use of exosomes as drug delivery systems. J Nanobiotechnology. 2018 Oct 16;16(1):81. doi: 10.1186/s12951-018-0403-9. PMID: 30326899; PMCID: PMC6190562.

Cañas JA, Rodrigo-Muñoz JM, Del Pozo V. Isolation and Functional Aspects of Eosinophil-Derived Exosomes. Methods Mol Biol. 2021; 2241:149-159. doi: 10.1007/978-1-0716-1095-4_13. PMID: 33486735.

Cañas JA, Sastre B, Rodrigo-Muñoz JM, Fernández-Nieto M, Barranco P, Quirce S, Sastre J, Del Pozo V. Eosinophil-derived exosomes contribute to asthma remodelling by activating structural lung cells. Clin Exp Allergy. 2018 Sep;48(9):1173-1185. doi: 10.1111/cea.13122. Epub 2018 Mar 8. PMID: 29451337.

Cañas JA, Sastre B, Mazzeo C, Fernández-Nieto M, Rodrigo-Muñoz JM, González-Guerra A, Izquierdo M, Barranco P, Quirce S, Sastre J, Del Pozo V. Exosomes from eosinophils autoregulate and promote eosinophil functions. J Leukoc Biol. 2017 May;101(5):1191-1199. doi: 10.1189/jlb.3AB0516-233RR. Epub 2017 Jan 17. PMID: 28096299.

Carretero R, Sektioglu IM, Garbi N, Salgado OC, Beckhove P, Hämmerling GJ. Eosinophils orchestrate cancer rejection by normalizing tumor vessels and enhancing infiltration of CD8(+) T cells. Nat Immunol. 2015 Jun;16(6):609-17. doi: 10.1038/ni.3159. Epub 2015 Apr 27. Erratum in: Nat Immunol. 2016 Feb;17(2):214. PMID: 25915731.

Cayrol C, Girard JP. Interleukin-33 (IL-33): A nuclear cytokine from the IL-1 family. Immunol Rev. 2018 Jan;281(1):154-168. doi: 10.1111/imr.12619. PMID: 29247993.

Chang CP, Hu MH, Hsiao YP, Wang YC. ST2 Signaling in the Tumor Microenvironment. Adv Exp Med Biol. 2020; 1240:83-93. doi: 10.1007/978-3-030-38315-2_7. PMID: 32060890.

Chen F, Chen J, Yang L, Liu J, Zhang X, Zhang Y, Tu Q, Yin D, Lin D, Wong PP, Huang D, Xing Y, Zhao J, Li M, Liu Q, Su F, Su S, Song E. Extracellular vesicle-packaged HIF-1α-stabilizing lncRNA from tumour-associated macrophages regulates aerobic glycolysis of breast cancer cells. Nat Cell Biol. 2019 Apr;21(4):498-510. doi: 10.1038/s41556-019-0299-0. Epub 2019 Apr 1. PMID: 30936474.

Chen L, Zhang YH, Wang S, Zhang Y, Huang T, Cai YD. Prediction and analysis of essential genes using the enrichments of gene ontology and KEGG pathways. PLoS One. 2017 Sep 5;12(9):e0184129. doi: 10.1371/journal.pone.0184129. PMID: 28873455; PMCID: PMC5584762.

Cho JA, Lee YS, Kim SH, Ko JK, Kim CW. MHC independent anti-tumor immune responses induced by Hsp70-enriched exosomes generate tumor regression in murine models. Cancer Lett. 2009 Mar 18;275(2):256-65. doi: 10.1016/j.canlet.2008.10.021. Epub 2008 Nov 25. PMID: 19036499.

Coscia C, Parolini I, Sanchez M, Biffoni M, Boussadia Z, Zanetti C, Fiani ML, Sargiacomo M. Generation, Quantification, and Tracing of Metabolically Labeled Fluorescent Exosomes. Methods Mol Biol. 2016; 1448:217-35. doi: 10.1007/978-1-4939-3753-0_16. PMID: 27317184.

Cui X, He Z, Liang Z, Chen Z, Wang H, Zhang J. Exosomes From Adipose-derived Mesenchymal Stem Cells Protect the Myocardium Against Ischemia/Reperfusion Injury Through Wnt/β-Catenin Signaling Pathway. J Cardiovasc Pharmacol. 2017 Oct;70(4):225-231. doi: 10.1097/FJC.0000000000000507. PMID: 28582278; PMCID: PMC5642342.

Deatherage BL, Cookson BT. Membrane vesicle release in bacteria, eukaryotes, and archaea: a conserved yet underappreciated aspect of microbial life. Infect Immun. 2012 Jun;80(6):1948-57. doi: 10.1128/IAI.06014-11. Epub 2012 Mar 12. PMID: 22409932; PMCID: PMC3370574.

Debnath P, Huirem RS, Dutta P, Palchaudhuri S. Epithelial-mesenchymal transition and its transcription factors. Biosci Rep. 2022 Jan 28;42(1): BSR20211754 doi: 10.1042/BSR20211754. PMID: 34708244; PMCID: PMC8703024.

Deng ZB, Liu Y, Liu C, Xiang X, Wang J, Cheng Z, Shah SV, Zhang S, Zhang L, Zhuang X, Michalek S, Grizzle WE, Zhang HG. Immature myeloid cells induced by a high-fat diet contribute to liver inflammation. Hepatology. 2009 Nov;50(5):1412-20. doi: 10.1002/hep.23148. PMID: 19708080; PMCID: PMC2852608.

Doyle LM, Wang MZ. Overview of Extracellular Vesicles, Their Origin, Composition, Purpose, and Methods for Exosome Isolation and Analysis. Cells. 2019 Jul 15;8(7):727. doi: 10.3390/cells8070727. PMID: 31311206; PMCID: PMC6678302.

Drake LY, Kita H. IL-33: biological properties, functions, and roles in airway disease. Immunol Rev. 2017 Jul;278(1):173-184. doi: 10.1111/imr.12552. PMID: 28658560; PMCID: PMC5492954.

Duault C, Betous D, Bezombes C, Roga S, Cayrol C, Girard JP, Fournié JJ, Poupot M. IL-33-expanded human Vγ9Vδ2 T cells have anti-lymphoma effect in a mouse tumor model. Eur J Immunol. 2017 Dec;47(12):2137-2141. doi: 10.1002/eji.201747093. Epub 2017 Sep 29. PMID: 28741710.

Enblad G, Sundstrom C, Glimelius B. Infiltration of eosinophils in Hodgkin's disease involved lymph nodes predicts prognosis. Hematol Oncol. 1993 Jul-Aug;11(4):187-93. doi: 10.1002/hon.2900110404. PMID: 8144133.

Engeland K. Cell cycle regulation: p53-p21-RB signaling. Cell Death Differ. 2022 May;29(5):946-960. doi: 10.1038/s41418-022-00988-z. Epub 2022 Mar 31. PMID: 35361964; PMCID: PMC9090780.

Ercolano G, Falquet M, Vanoni G, Trabanelli S, Jandus C. ILC2s: New Actors in Tumor Immunity. Front Immunol. 2019 Dec 3;10:2801. doi: 10.3389/fimmu.2019.02801. PMID: 31849977; PMCID: PMC6902088.

Essandoh K, Yang L, Wang X, Huang W, Qin D, Hao J, Wang Y, Zingarelli B, Peng T, Fan GC. Blockade of exosome generation with GW4869 dampens the sepsis-induced inflammation and cardiac dysfunction. BiochimBiophys Acta. 2015 Nov;1852(11):2362-71. doi: 10.1016/j.bbadis.2015.08.010. Epub 2015 Aug 20. PMID: 26300484; PMCID: PMC4581992.

Evan GI, Vousden KH. Proliferation, cell cycle and apoptosis in cancer. Nature. 2001 May 17;411(6835):342-8. doi: 10.1038/35077213. PMID: 11357141.

Filipazzi P, Bürdek M, Villa A, Rivoltini L, Huber V. Recent advances on the role of tumor exosomes in immunosuppression and disease progression. Semin Cancer Biol. 2012 Aug;22(4):342-9. doi: 10.1016/j.semcancer.2012.02.005. Epub 2012 Feb 19. PMID: 22369922.

Gao K, Li X, Zhang L, Bai L, Dong W, Gao K, Shi G, Xia X, Wu L, Zhang L. Transgenic expression of IL-33 activates CD8(+) T cells and NK cells and inhibits tumor growth and metastasis in mice. Cancer Lett. 2013 Jul 28;335(2):463-71. doi: 10.1016/j.canlet.2013.03.002. Epub 2013 Mar 14. PMID: 23499895.

Ge L, Zhang N, Li D, Wu Y, Wang H, Wang J. Circulating exosomal small RNAs are promising non-invasive diagnostic biomarkers for gastric cancer. J Cell Mol Med. 2020 Dec;24(24):14502-14513. doi: 10.1111/jcmm.16077. Epub 2020 Nov 9. PMID: 33169519; PMCID: PMC7753781.

Ghaffari S, Rezaei N. Eosinophils in the tumor microenvironment: implications for cancer immunotherapy. J Transl Med. 2023 Aug 16;21(1):551. doi: 10.1186/s12967-023-04418-7. PMID: 37587450; PMCID: PMC10433623.

Goedhart J, Luijsterburg MS. VolcaNoseR is a web app for creating, exploring, labeling and sharing volcano plots. Sci Rep. 2020 Nov 25;10(1):20560. doi: 10.1038/s41598-020-76603-3. PMID: 33239692; PMCID: PMC7689420.

Grisaru-Tal S, Dulberg S, Beck L, Zhang C, Itan M, Hediyeh-Zadeh S, Caldwell J, Rozenberg P, Dolitzky A, Avlas S, Hazut I, Gordon Y, Shani O, Tsuriel S, Gerlic M, Erez N, Jacquelot N, Belz GT, Rothenberg ME, Davis MJ, Yu H, Geiger T, Madi A, Munitz A. Metastasis-Entrained Eosinophils Enhance Lymphocyte-Mediated Antitumor Immunity. Cancer Res. 2021 Nov 1;81(21):5555-5571. doi: 10.1158/0008-5472.CAN-21-0839. Epub 2021 Aug 24. PMID: 34429328.

Guan S, Li Q, Liu P, Xuan X, Du Y. Umbilical cord blood-derived dendritic cells loaded with BGC823 tumor antigens and DC-derived exosomes stimulate efficient cytotoxic T-lymphocyte responses and antitumor immunity in vitro and in vivo. Cent Eur J Immunol. 2014;39(2):142-51. doi: 10.5114/ceji.2014.43713. Epub 2014 Jun 27. PMID: 26155115; PMCID: PMC4440031.

Gurung S, Perocheau D, Touramanidou L, Baruteau J. The exosome journey: from biogenesis to uptake and intracellular signalling. Cell Commun Signal. 2021 Apr 23;19(1):47. doi: 10.1186/s12964-021-00730-1. PMID: 33892745; PMCID: PMC8063428.

Ha D, Yang N, Nadithe V. Exosomes as therapeutic drug carriers and delivery vehicles across biological membranes: current perspectives and future challenges. Acta Pharm Sin B. 2016 Jul;6(4):287-96. doi: 10.1016/j.apsb.2016.02.001. Epub 2016 Mar 8. PMID: 27471669; PMCID: PMC4951582.

Han J, Zhao G, Ma X, Dong Q, Zhang H, Wang Y, Cui J. CircRNA circ-BANP-mediated miR-503/LARP1 signaling contributes to lung cancer progression. BiochemBiophys Res Commun. 2018 Sep 18;503(4):2429-2435. doi: 10.1016/j.bbrc.2018.06.172. Epub 2018 Jul 6. PMID: 29969631.

Haney MJ, Klyachko NL, Zhao Y, Gupta R, Plotnikova EG, He Z, Patel T, Piroyan A, Sokolsky M, Kabanov AV, Batrakova EV. Exosomes as drug delivery vehicles for Parkinson's disease therapy. J Control Release. 2015 Jun 10;207:18-30. doi: 10.1016/j.jconrel.2015.03.033. Epub 2015 Mar 31. Erratum in: J Control Release. 2021 Nov 10;339:232-234. PMID: 25836593; PMCID: PMC4430381.

Hogan SP, Rosenberg HF, Moqbel R, Phipps S, Foster PS, Lacy P, Kay AB, Rothenberg ME. Eosinophils: biological properties and role in health and disease. Clin Exp Allergy. 2008 May;38(5):709-50. doi: 10.1111/j.1365-2222.2008.02958.x.Epub 2008 Apr 1. PMID: 18384431.

Hood JL, San RS, Wickline SA. Exosomes released by melanoma cells prepare sentinel lymph nodes for tumor metastasis. Cancer Res. 2011 Jun 1;71(11):3792-801. doi: 10.1158/0008-5472.CAN-10-4455. Epub 2011 Apr 8. PMID: 21478294.

Horibe S, Tanahashi T, Kawauchi S, Murakami Y, Rikitake Y. Mechanism of recipient cell-dependent differences in exosome uptake. BMC Cancer. 2018 Jan 6;18(1):47. doi: 10.1186/s12885-017-3958-1. PMID: 29306323; PMCID: PMC5756423.

Howitt J, Hill AF. Exosomes in the Pathology of Neurodegenerative Diseases. J Biol Chem. 2016 Dec 23;291(52):26589-26597. doi: 10.1074/jbc.R116.757955. Epub 2016 Nov 16. PMID: 27852825; PMCID: PMC5207170.

Huber V, Fais S, Iero M, Lugini L, Canese P, Squarcina P, Zaccheddu A, Colone M, Arancia G, Gentile M, Seregni E, Valenti R, Ballabio G, Belli F, Leo E, Parmiani G, Rivoltini L. Human colorectal cancer cells induce T-cell death through release of proapoptotic microvesicles: role in immune escape. Gastroenterology. 2005 Jun;128(7):1796-804. doi: 10.1053/j.gastro.2005.03.045. PMID: 15940614.

Hume S, Grou CP, Lascaux P, D'Angiolella V, Legrand AJ, Ramadan K, Dianov GL. The NUCKS1-SKP2-p21/p27 axis controls S phase entry. Nat Commun. 2021 Nov 29;12(1):6959. doi: 10.1038/s41467-021-27124-8. PMID: 34845229; PMCID: PMC8630071.

Ji F, Sadreyev RI. RNA-seq: Basic Bioinformatics Analysis. CurrProtoc Mol Biol. 2018 Oct;124(1):e68. doi: 10.1002/cpmb.68. Epub 2018 Sep 17. PMID: 30222249; PMCID: PMC6168365.

Jia S, Li W, Liu P, Xu LX. A role of eosinophils in mediating the anti-tumour effect of cryo-thermal treatment. Sci Rep. 2019 Sep 13;9(1):13214. doi: 10.1038/s41598-019-49734-5. PMID: 31519961; PMCID: PMC6744470.

Joshi BS, de Beer MA, Giepmans BNG, Zuhorn IS. Endocytosis of Extracellular Vesicles and Release of Their Cargo from Endosomes. ACS Nano. 2020 Apr 28;14(4):4444-4455. doi: 10.1021/acsnano.9b10033. Epub 2020 Apr 16. PMID: 32282185; PMCID: PMC7199215.

Jovanovic IP, Pejnovic NN, Radosavljevic GD, Pantic JM, Milovanovic MZ, Arsenijevic NN, Lukic ML. Interleukin-33/ST2 axis promotes breast cancer growth and metastases by

facilitating intratumoral accumulation of immunosuppressive and innate lymphoid cells. Int J Cancer. 2014 Apr 1;134(7):1669-82. doi: 10.1002/ijc.28481. Epub 2013 Oct 10. PMID: 24105680.

Kalluri R. The biology and function of exosomes in cancer. J Clin Invest. 2016 Apr 1;126(4):1208-15. doi: 10.1172/JCI81135. Epub 2016 Apr 1. PMID: 27035812; PMCID: PMC4811149.

Kim MS, Kim E, Heo JS, Bae DJ, Lee JU, Lee TH, Lee HJ, Chang HS, Park JS, Jang AS, Koh ES, Hwang HG, Lim G, Kim S, Park CS. Circulating IL-33 level is associated with the progression of lung cancer. Lung Cancer. 2015 Nov;90(2):346-51. doi: 10.1016/j.lungcan.2015.08.011. Epub 2015 Aug 20. PMID: 26342550.

Kolberg L, Raudvere U, Kuzmin I, Adler P, Vilo J, Peterson H. g:Profiler-interoperable web service for functional enrichment analysis and gene identifier mapping (2023 update). Nucleic Acids Res. 2023 Jul 5;51(W1):W207-W212. doi: 10.1093/nar/gkad347. PMID: 37144459; PMCID: PMC10320099.

Kvarnhammar AM, Cardell LO. Pattern-recognition receptors in human eosinophils. Immunology. 2012 May;136(1):11-20. doi: 10.1111/j.1365-2567.2012.03556.x. PMID: 22242941; PMCID: PMC3372752.

Lakhal S, Wood MJ. Exosome nanotechnology: an emerging paradigm shift in drug delivery: exploitation of exosome nanovesicles for systemic in vivo delivery of RNAi heralds new horizons for drug delivery across biological barriers. Bioessays. 2011 Oct;33(10):737-41. doi: 10.1002/bies.201100076. PMID: 21932222.

Lan J, Sun L, Xu F, Liu L, Hu F, Song D, Hou Z, Wu W, Luo X, Wang J, Yuan X, Hu J, Wang G. M2 Macrophage-Derived Exosomes Promote Cell Migration and Invasion in Colon Cancer. Cancer Res. 2019 Jan 1;79(1):146-158. doi: 10.1158/0008-5472.CAN-18-0014. Epub 2018 Nov 6. PMID: 30401711.

Lau NCH, Yam JWP. From Exosome Biogenesis to Absorption: Key Takeaways for Cancer Research. Cancers (Basel). 2023 Mar 27;15(7):1992. doi: 10.3390/cancers15071992. PMID: 37046653; PMCID: PMC10093369.

Leal-Esteban LC, Fajas L. Cell cycle regulators in cancer cell metabolism. BiochimBiophys Acta Mol Basis Dis. 2020 May 1;1866(5):165715. doi: 10.1016/j.bbadis.2020.165715. Epub 2020 Feb 5. PMID: 32035102.

Liang Y, Duan L, Lu J, Xia J. Engineering exosomes for targeted drug delivery. Theranostics. 2021 Jan 1;11(7):3183-3195. doi: 10.7150/thno.52570. PMID: 33537081; PMCID: PMC7847680.

Liebl MC, Hofmann TG. The Role of p53 Signaling in Colorectal Cancer. Cancers (Basel). 2021 Apr 28;13(9):2125. doi: 10.3390/cancers13092125. PMID: 33924934; PMCID: PMC8125348.

Liew FY, Girard JP, Turnquist HR. Interleukin-33 in health and disease. Nat Rev Immunol. 2016 Nov;16(11):676-689. doi: 10.1038/nri.2016.95. Epub 2016 Sep 19. PMID: 27640624.

Liu J, Peng Y, Wei W. Cell cycle on the crossroad of tumorigenesis and cancer therapy. Trends Cell Biol. 2022 Jan;32(1):30-44. doi: 10.1016/j.tcb.2021.07.001. Epub 2021 Jul 22. PMID: 34304958; PMCID: PMC8688170.

Loh CY, Chai JY, Tang TF, Wong WF, Sethi G, Shanmugam MK, Chong PP, Looi CY. The E-Cadherin and N-Cadherin Switch in Epithelial-to-Mesenchymal Transition: Signaling, Therapeutic Implications, and Challenges. Cells. 2019 Sep 20;8(10):1118. doi: 10.3390/cells8101118. PMID: 31547193; PMCID: PMC6830116.

Lu W, Kang Y. Epithelial-Mesenchymal Plasticity in Cancer Progression and Metastasis. Dev Cell. 2019 May 6;49(3):361-374. doi: 10.1016/j.devcel.2019.04.010. PMID: 31063755; PMCID: PMC6506183.

Lu J, Kang J, Zhang C, Zhang X. The role of IL-33/ST2L signals in the immune cells. Immunol Lett. 2015 Mar;164(1):11-7. doi: 10.1016/j.imlet.2015.01.008. Epub 2015 Feb 4. PMID: 25662624.

Lucarini V, Buccione C, Zicchedda G, Peschiaroli F, Sestili P, Puglisi R, Mattia G, Zanetti C, Parolini I, Bracci L, Macchia I, Rossi A, D'Urso MT, Macchia D, Spada M, De Ninno A, Gerardino A, Mozetic P, Trombetta M, Rainer A, Businaro L, Schiavoni G, Mattei F. CombiningType I Interferons and 5-Aza-2'-Deoxycitidine to Improve Anti-TumorResponseagainst Melanoma. J Invest Dermatol. 2017 Jan;137(1):159-169. doi: 10.1016/j.jid.2016.08.024. Epub 2016 Sep 10. PMID: 27623509.

Mallegol J, Van Niel G, Lebreton C, Lepelletier Y, Candalh C, Dugave C, Heath JK, Raposo G, Cerf-Bensussan N, Heyman M. T84-intestinal epithelial exosomes bear MHC class II/peptide complexes potentiating antigen presentation by dendritic cells. Gastroenterology. 2007 May;132(5):1866-76. doi: 10.1053/j.gastro.2007.02.043. Epub 2007 Feb 22. PMID: 17484880.

Marone G, Gambardella AR, Mattei F, Mancini J, Schiavoni G, Varricchi G. Basophils in Tumor Microenvironment and Surroundings. Adv Exp Med Biol. 2020;1224:21-34. doi: 10.1007/978-3-030-35723-8_2. PMID: 32036602.

Marone G, Schroeder JT, Mattei F, Loffredo S, Gambardella AR, Poto R, de Paulis A, Schiavoni G, Varricchi G. Is There a Role for Basophils in Cancer? Front Immunol. 2020 Sep 8;11:2103. doi: 10.3389/fimmu.2020.02103. PMID: 33013885; PMCID: PMC7505934.

Mashouri L, Yousefi H, Aref AR, Ahadi AM, Molaei F, Alahari SK. Exosomes: composition, biogenesis, and mechanisms in cancer metastasis and drug resistance. Mol Cancer. 2019 Apr 2;18(1):75. doi: 10.1186/s12943-019-0991-5. PMID: 30940145; PMCID: PMC6444571.

Mazzeo C, Cañas JA, Zafra MP, Rojas Marco A, Fernández-Nieto M, Sanz V, Mittelbrunn M, Izquierdo M, Baixaulli F, Sastre J, Del Pozo V. Exosome secretion by eosinophils: A possible role in asthma pathogenesis. J Allergy Clin Immunol. 2015 Jun;135(6):1603-13. doi: 10.1016/j.jaci.2014.11.026. Epub 2015 Jan 21. PMID: 25617225.

Men Y, Yelick J, Jin S, Tian Y, Chiang MSR, Higashimori H, Brown E, Jarvis R, Yang Y. Exosome reporter mice reveal the involvement of exosomes in mediating neuron to astroglia communication in the CNS. Nat Commun. 2019 Sep 12;10(1):4136. doi: 10.1038/s41467-019-11534-w. PMID: 31515491; PMCID: PMC6742670.

Morita E, Sandrin V, Chung HY, Morham SG, Gygi SP, Rodesch CK, Sundquist WI. Human ESCRT and ALIX proteins interact with proteins of the midbody and function in cytokinesis. EMBO J. 2007 Oct 3;26(19):4215-27. doi: 10.1038/sj.emboj.7601850. Epub 2007 Sep 13. Erratum in: EMBO J. 2012 Jul 18;31(14):3228. PMID: 17853893; PMCID: PMC2230844.

Murphy DE, de Jong OG, Brouwer M, Wood MJ, Lavieu G, Schiffelers RM, Vader P. Extracellular vesicle-based therapeutics: natural versus engineered targeting and trafficking.

Exp Mol Med. 2019 Mar 15;51(3):1-12. doi: 10.1038/s12276-019-0223-5. PMID: 30872574; PMCID: PMC6418170.

Nolte-'t Hoen EN, Buschow SI, Anderton SM, Stoorvogel W, Wauben MH. Activated T cells recruit exosomes secreted by dendritic cells via LFA-1. Blood. 2009 Feb 26;113(9):1977-81. doi: 10.1182/blood-2008-08-174094. Epub 2008 Dec 8. Erratum in: Blood. 2009 Sep 24;114(13):2851. PMID: 19064723.

O'Brien K, Ughetto S, Mahjoum S, Nair AV, Breakefield XO. Uptake, functionality, and re-release of extracellular vesicle-encapsulated cargo. Cell Rep. 2022 Apr 12;39(2):110651. doi: 10.1016/j.celrep.2022.110651. PMID: 35417683; PMCID: PMC9074118.

Oliveira SH, Lukacs NW. The role of chemokines and chemokine receptors in eosinophil activation during inflammatory allergic reactions. Braz J Med Biol Res. 2003 Nov;36(11):1455-63. doi: 10.1590/s0100-879x2003001100002. Epub 2003 Oct 22. PMID: 14576899.

Osaki M, Okada F. Exosomes and Their Role in Cancer Progression. Yonago Acta Med. 2019 Jun 20;62(2):182-190. doi: 10.33160/yam.2019.06.002. PMID: 31320822; PMCID: PMC6584259.

Parolini I, Federici C, Raggi C, Lugini L, Palleschi S, De Milito A, Coscia C, Iessi E, Logozzi M, Molinari A, Colone M, Tatti M, Sargiacomo M, Fais S. Microenvironmental pH is a key factor for exosometraffic in tumorcells. J Biol Chem. 2009 Dec 4;284(49):34211-22. doi: 10.1074/jbc.M109.041152. Epub 2009 Sep 30. PMID: 19801663; PMCID: PMC2797191.

Perez-Hernandez D, Gutiérrez-Vázquez C, Jorge I, López-Martín S, Ursa A, Sánchez-Madrid F, Vázquez J, Yáñez-Mó M. The intracellular interactome of tetraspanin-enriched microdomains reveals their function as sorting machineries toward exosomes. J Biol Chem. 2013 Apr 26;288(17):11649-61. doi: 10.1074/jbc.M112.445304. Epub 2013 Mar 5. PMID: 23463506; PMCID: PMC3636856.

Phipps S, Lam CE, Mahalingam S, Newhouse M, Ramirez R, Rosenberg HF, Foster PS, Matthaei KI. Eosinophils contribute to innate antiviral immunity and promote clearance of respiratory syncytial virus. Blood. 2007 Sep 1;110(5):1578-86. doi: 10.1182/blood-2007-01-071340. Epub 2007 May 10. PMID: 17495130.

Qin L, Dominguez D, Chen S, Fan J, Long A, Zhang M, Fang D, Zhang Y, Kuzel TM, Zhang B. Exogenous IL-33 overcomes T cell tolerance in murine acute myeloid leukemia. Oncotarget. 2016 Sep 20;7(38):61069-61080. doi: 10.18632/oncotarget.11179. PMID: 27517629; PMCID: PMC5308636.

Ramadhani HF, Annisa A, Tedjo A, Noor DR, Kusuma WA. Combination of Enrichment Using Gene Ontology and Transcriptomic Analysis Revealed Contribution of Interferon Signaling to Severity of COVID-19. InterdiscipPerspect Infect Dis. 2022 Apr 11;2022:3515001. doi: 10.1155/2022/3515001. PMID: 35422859; PMCID: PMC9002903.

Ratajczak J, Miekus K, Kucia M, Zhang J, Reca R, Dvorak P, Ratajczak MZ. Embryonic stem cell-derived microvesicles reprogram hematopoietic progenitors: evidence for horizontal transfer of mRNA and protein delivery. Leukemia. 2006 May;20(5):847-56. doi: 10.1038/sj.leu.2404132. PMID: 16453000.

Reichman H, Itan M, Rozenberg P, Yarmolovski T, Brazowski E, Varol C, Gluck N, Shapira S, Arber N, Qimron U, Karo-Atar D, Lee JJ, Munitz A. Activated Eosinophils Exert Antitumorigenic Activities in Colorectal Cancer. Cancer Immunol Res. 2019 Mar;7(3):388-400. doi: 10.1158/2326-6066.CIR-18-0494. Epub 2019 Jan 21. PMID: 30665890.

Rodrigo-Muñoz JM, Cañas JA, Sastre B, Gil-Martínez M, García Latorre R, Sastre J, Del Pozo V. Role of miR-185-5p as modulator of periostin synthesis and smooth muscle contraction in asthma. J Cell Physiol. 2022 Feb;237(2):1498-1508. doi: 10.1002/jcp.30620. Epub 2021 Oct 26. PMID: 34698372; PMCID: PMC9298424.

Rosenberg HF, Dyer KD, Foster PS. Eosinophils: changing perspectives in health and disease. Nat Rev Immunol. 2013 Jan;13(1):9-22. doi: 10.1038/nri3341. Epub 2012 Nov 16. PMID: 23154224; PMCID: PMC4357492.

Roussel L, Erard M, Cayrol C, Girard JP. Molecular mimicry between IL-33 and KSHV for attachment to chromatin through the H2A-H2B acidic pocket. EMBO Rep. 2008 Oct;9(10):1006-12. doi: 10.1038/embor.2008.145. Epub 2008 Aug 8. PMID: 18688256; PMCID: PMC2572127.

Ruiss R, Jochum S, Mocikat R, Hammerschmidt W, Zeidler R. EBV-gp350 confers B-cell tropism to tailored exosomes and is a neo-antigen in normal and malignant B cells--a new option for the treatment of B-CLL. PLoS One. 2011;6(10):e25294. doi: 10.1371/journal.pone.0025294. Epub 2011 Oct 10. PMID: 22022385; PMCID: PMC3189918.

Santos MF, Rappa G, Karbanová J, Kurth T, Corbeil D, Lorico A. VAMP-associated protein-A and oxysterol-binding protein-related protein 3 promote the entry of late endosomes into the nucleoplasmic reticulum. J Biol Chem. 2018 Sep 7;293(36):13834-13848. doi: 10.1074/jbc.RA118.003725. Epub 2018 Jul 17. PMID: 30018135; PMCID: PMC6130944.

Shamri R, Xenakis JJ, Spencer LA. Eosinophils in innate immunity: an evolving story. Cell Tissue Res. 2011 Jan;343(1):57-83. doi: 10.1007/s00441-010-1049-6. Epub 2010 Nov 3. PMID: 21042920; PMCID: PMC3679536.

Simon SCS, Hu X, Panten J, Grees M, Renders S, Thomas D, Weber R, Schulze TJ, Utikal J, Umansky V. Eosinophil accumulation predicts response to melanoma treatment with immune checkpoint inhibitors. Oncoimmunology. 2020 Feb 15;9(1):1727116. doi: 10.1080/2162402X.2020.1727116. PMID: 32117594; PMCID: PMC7028332.

Simon SCS, Utikal J, Umansky V. Opposing roles of eosinophils in cancer. Cancer Immunol Immunother. 2019 May;68(5):823-833. doi: 10.1007/s00262-018-2255-4. Epub 2018 Oct 9. PMID: 30302498.

Skotland T, Hessvik NP, Sandvig K, Llorente A. Exosomal lipid composition and the role of ether lipids and phosphoinositides in exosome biology. J Lipid Res. 2019 Jan;60(1):9-18. doi: 10.1194/jlr.R084343. Epub 2018 Aug 3. PMID: 30076207; PMCID: PMC6314266.

Skryabin GO, Komelkov AV, Savelyeva EE, Tchevkina EM. Lipid Rafts in Exosome Biogenesis. Biochemistry (Mosc). 2020 Feb;85(2):177-191. doi: 10.1134/S0006297920020054. PMID: 32093594.

Spits H, Artis D, Colonna M, Diefenbach A, Di Santo JP, Eberl G, Koyasu S, Locksley RM, McKenzie AN, Mebius RE, Powrie F, Vivier E. Innate lymphoid cells--a proposal for uniform nomenclature. Nat Rev Immunol. 2013 Feb;13(2):145-9. doi: 10.1038/nri3365. PMID: 23348417.

Tauro BJ, Greening DW, Mathias RA, Ji H, Mathivanan S, Scott AM, Simpson RJ. Comparison of ultracentrifugation, density gradient separation, and immunoaffinity capture methods for isolating human colon cancer cell line LIM1863-derived exosomes. Methods. 2012 Feb;56(2):293-304. doi: 10.1016/j.ymeth.2012.01.002. Epub 2012 Jan 21. PMID: 22285593.

Thomou T, Mori MA, Dreyfuss JM, Konishi M, Sakaguchi M, Wolfrum C, Rao TN, Winnay JN, Garcia-Martin R, Grinspoon SK, Gorden P, Kahn CR. Adipose-derived circulating miRNAs regulate gene expression in other tissues. Nature. 2017 Feb 23;542(7642):450-455. doi: 10.1038/nature21365. Epub 2017 Feb 15. Erratum in: Nature. 2017 May 10;545(7653):252. PMID: 28199304; PMCID: PMC5330251.

Tian T, Zhu YL, Hu FH, Wang YY, Huang NP, Xiao ZD. Dynamics of exosome internalization and trafficking. J Cell Physiol. 2013 Jul;228(7):1487-95. doi: 10.1002/jcp.24304. PMID: 23254476.

Trajkovic K, Hsu C, Chiantia S, Rajendran L, Wenzel D, Wieland F, Schwille P, Brügger B, Simons M. Ceramide triggers budding of exosome vesicles into multivesicular endosomes. Science. 2008 Feb 29;319(5867):1244-7. doi: 10.1126/science.1153124. PMID: 18309083.

Tung SL, Boardman DA, Sen M, Letizia M, Peng Q, Cianci N, Dioni L, Carlin LM, Lechler R, Bollati V, Lombardi G, Smyth LA. Regulatory T cell-derived extracellular vesicles modify dendritic cell function. Sci Rep. 2018 Apr 17;8(1):6065. doi: 10.1038/s41598-018-24531-8. PMID: 29666503; PMCID: PMC5904112.

Utsunomiya A, Ishida T, Inagaki A, Ishii T, Yano H, Komatsu H, Iida S, Yonekura K, Takeuchi S, Takatsuka Y, Ueda R. Clinical significance of a blood eosinophilia in adult T-cell leukemia/lymphoma: a blood eosinophilia is a significant unfavorable prognostic factor. Leuk Res. 2007 Jul;31(7):915-20. doi: 10.1016/j.leukres.2006.10.017. Epub 2006 Nov 22. PMID: 17123603.

Valadi H, Ekström K, Bossios A, Sjöstrand M, Lee JJ, Lötvall JO. Exosome-mediated transfer of mRNAs and microRNAs is a novel mechanism of genetic exchange between cells. Nat Cell Biol. 2007 Jun;9(6):654-9. doi: 10.1038/ncb1596. Epub 2007 May 7. PMID: 17486113.

Varricchi G, Galdiero MR, Loffredo S, Lucarini V, Marone G, Mattei F, Marone G, Schiavoni G. Eosinophils: The unsungheroes in cancer? Oncoimmunology. 2017 Nov 13;7(2):e1393134. doi: 10.1080/2162402X.2017.1393134. PMID: 29308325; PMCID: PMC5749653.

Varricchi G, Galdiero MR, Loffredo S, Marone G, Iannone R, Marone G, Granata F. Are MastCellsMASTers in Cancer? Front Immunol. 2017 Apr 12;8:424. doi: 10.3389/fimmu.2017.00424. PMID: 28446910; PMCID: PMC5388770.

Villarreal DO, Wise MC, Walters JN, Reuschel EL, Choi MJ, Obeng-Adjei N, Yan J, Morrow MP, Weiner DB. Alarmin IL-33 acts as an immunoadjuvant to enhance antigen-specific tumor immunity. Cancer Res. 2014 Mar 15;74(6):1789-800. doi: 10.1158/0008-5472.CAN-13-2729. Epub 2014 Jan 21. PMID: 24448242; PMCID: PMC4130175.

Von Wasielewski R, Seth S, Franklin J, Fischer R, Hübner K, Hansmann ML, Diehl V, Georgii A. Tissue eosinophilia correlates strongly with poor prognosis in nodular sclerosing Hodgkin's disease, allowing for known prognostic factors. Blood. 2000 Feb 15;95(4):1207-13. PMID: 10666192.

Wenes M, Shang M, Di Matteo M, Goveia J, Martín-Pérez R, Serneels J, Prenen H, Ghesquière B, Carmeliet P, Mazzone M. Macrophage Metabolism Controls Tumor Blood Vessel Morphogenesis and Metastasis. Cell Metab. 2016 Nov 8;24(5):701-715. doi: 10.1016/j.cmet.2016.09.008. Epub 2016 Oct 20. PMID: 27773694.

Xie F, Liu LB, Shang WQ, Chang KK, Meng YH, Mei J, Yu JJ, Li DJ, Li MQ. The infiltration and functional regulation of eosinophils induced by TSLP promote the proliferation of cervical

cancer cell. Cancer Lett. 2015 Aug 10;364(2):106-17. doi: 10.1016/j.canlet.2015.04.029. Epub 2015 May 12. PMID: 25979231.

Xiong J, Chi H, Yang G, Zhao S, Zhang J, Tran LJ, Xia Z, Yang F, Tian G. Revolutionizing anti-tumor therapy: unleashing the potential of B cell-derived exosomes. Front Immunol. 2023 Jun 5;14:1188760. doi: 10.3389/fimmu.2023.1188760. PMID: 37342327; PMCID: PMC10277631.

Yan W, Jiang S. Immune Cell-Derived Exosomes in the Cancer-Immunity Cycle. Trends Cancer. 2020 Jun;6(6):506-517. doi: 10.1016/j.trecan.2020.02.013. Epub 2020 Mar 17. PMID: 32460004.

Yang E, Wang X, Gong Z, Yu M, Wu H, Zhang D. Exosome-mediated metabolic reprogramming: the emerging role in tumor microenvironment remodeling and its influence on cancer progression. Signal Transduct Target Ther. 2020 Oct 19;5(1):242. doi: 10.1038/s41392-020-00359-5. PMID: 33077737; PMCID: PMC7572387.

Yang M, Feng Y, Yue C, Xu B, Chen L, Jiang J, Lu B, Zhu Y. Lower expression level of IL-33 is associated with poor prognosis of pulmonary adenocarcinoma. PLoS One. 2018 Mar 2;13(3):e0193428. doi: 10.1371/journal.pone.0193428. PMID: 29499051; PMCID: PMC5834175.

Yao Y, Zuo J, Wei Y. Targeting of TRX2 by miR-330-3p in melanoma inhibits proliferation. Biomed Pharmacother. 2018 Nov;107:1020-1029. doi: 10.1016/j.biopha.2018.08.058. Epub 2018 Aug 24. PMID: 30257313.

Zamani P, Fereydouni N, Butler AE, Navashenaq JG, Sahebkar A. The therapeutic and diagnostic role of exosomes in cardiovascular diseases. Trends Cardiovasc Med. 2019 Aug;29(6):313-323. doi: 10.1016/j.tcm.2018.10.010. Epub 2018 Oct 24. PMID: 30385010.

Zech D, Rana S, Büchler MW, Zöller M. Tumor-exosomes and leukocyte activation: an ambivalent crosstalk. Cell Commun Signal. 2012 Nov 28;10(1):37. doi: 10.1186/1478-811X-10-37. PMID: 23190502; PMCID: PMC3519567.

Zhang B, Wang M, Gong A, Zhang X, Wu X, Zhu Y, Shi H, Wu L, Zhu W, Qian H, Xu W. HucMSC-Exosome Mediated-Wnt4 Signaling Is Required for Cutaneous Wound Healing. Stem Cells. 2015 Jul;33(7):2158-68. doi: 10.1002/stem.1771. Epub 2015 May 13. Erratum in: Stem Cells. 2021 Dec;39(12):E5. PMID: 24964196.

Zhang L, Yu D. Exosomes in cancer development, metastasis, and immunity. BiochimBiophys Acta Rev Cancer. 2019 Apr;1871(2):455-468. doi: 10.1016/j.bbcan.2019.04.004. Epub 2019 Apr 30. PMID: 31047959; PMCID: PMC6542596.

Zhang Y, Liu Y, Liu H, Tang WH. Exosomes: biogenesis, biologic function and clinical potential. Cell Biosci. 2019 Feb 15;9:19. doi: 10.1186/s13578-019-0282-2. PMID: 30815248; PMCID: PMC6377728.

Zhao P, Guo S, Tu Z, Di L, Zha X, Zhou H, Zhang X. Grhl3 induces human epithelial tumor cell migration and invasion via downregulation of E-cadherin. Acta BiochimBiophys Sin (Shanghai). 2016 Mar;48(3):266-74. doi: 10.1093/abbs/gmw001. Epub 2016 Feb 1. PMID: 26837418; PMCID: PMC4885135.

Zhou Y, Zhang Y, Gong H, Luo S, Cui Y. The Role of Exosomes and Their Applications in Cancer. Int J Mol Sci. 2021 Nov 11;22(22):12204. doi: 10.3390/ijms222212204. PMID: 34830085; PMCID: PMC8622108.